Optimization of Exhaust Port and Valve to improve exhaust flow for heavy duty engines.

Master's Thesis

By

Gokul Kanna Balakrishnan

Department of Energy Sciences

Faculty of Engineering, LTH, Lund University

June 2024

LUND UNIVERSITY

Academic Supervisor: Per Tunestål

Company Supervisor: Ulf Aronsson, Volvo GTT

Examiner: Martin Tuner

VOLVO

1. Table of Contents

List of Figures

2. Abbreviations

CFD- Computational Fluid Dynamics

CAD- Computer Aided Design

ICE- Internal Combustion Engine

PMEP- Pumping Mean Effective Pressure

FMEP- Friction Mean Effective Pressure

HTMEP- Heat Transfer Mean Effective Pressure

ExMEP- Exhaust Heat Mean Effective Pressure

RANS- Reynolds Averaged Navier Stokes

LES- Large Eddy Simulation

DES- Detached Eddy Simulation

3. Popular Science Summary

Internal combustion engines are majorly used in transportation sectors. Throughout the years ICE have undergone significant developments in terms of being more efficient, reliable and to reduce emissions. Even with this level of advancements, losses are still a huge factor. One such loss is pumping loss. Exhaust gases contain a significant portion of energy after combustion and need to be pushed out of the combustion chamber. Improper flow of exhaust gases can lead to combustion problems and drop in efficiency due to retention of exhaust gas in the chamber. However, the exhaust gases are not entirely able to move out of the combustion chamber which causes the piston to use some work to push the gases out. This work done by piston is the pumping work.

This master's thesis focuses on the optimization of the exhaust port geometry to improve the exhaust gas flow to reduce blowdown losses. Using advanced computational fluid dynamics (CFD) software Star CCM+, analysis of different designs and its influence on the flow of exhaust gases. The goal is to identify and implement design changes that maximize the exhaust gas flow and to analyze the improvements in efficiency.

Efficient exhaust gas flow is crucial for the performance and environmental impact of internal combustion engines. This project investigates how modifying the geometry of exhaust ports can enhance the flow of exhaust gases, reducing pressure losses and improving overall engine efficiency. By employing CFD simulations and optimization techniques, the study seeks to identify and implement design changes that offer significant performance improvements. The findings of this research could lead to the development of more advanced, cleaner engines.

The results indicate that modifying the exhaust port to have a gradual expansion area can lead to good improvement in exhaust flow. On the other hand, it is impossible to make a large improvement in flow without modifying the valve geometry. Also, even with the best improvement in exhaust flow the efficiency does not correspond to the same amount of improvement.

4. Abstract

The efficiency of combustion engines is crucial for their future development, prompting researchers to explore various factors to enhance performance. Among these factors, exhaust gases hold significant potential. Typically, exhaust gases carry about 30-40% of the engine's energy, which often remains underutilized. Although technologies like turbochargers have made progress in recovering some of this lost energy, a considerable amount is still lost due to the energy required to expel the exhaust gases from the combustion chamber.

This thesis aims to improve the flow in the exhaust port of a 13L Volvo engine by using optimization strategies. STAR CCM+ is used for steady state computational fluid dynamics (CFD) analysis, focusing on flow and pressure losses at various valve lifts.

Different optimization strategies were analyzed and among that parameter optimization was the best suited for this thesis. Parameter optimization aims at modifying parameters like radius, angle, area. Several parameters were modified to the exhaust port and valves and tested to identify the most effective improvements. Four cases were performed to analyze the performance. In case 1, aligning the valve face with the cylinder head showed flow improvement at certain valve lifts, but overall, the performance was similar to the base geometry. In case 2, with the port positioned above the cylinder head, resulted in deteriorated flow after a few lifts. Case 3, which involved enlarging the port neck area, and case 4, which involved smoothing the valve edges along with case 3, showed improvements in flow by 5.3% and 6.9%, respectively. However, the fourth modification posed complications due to a reduced valve seat area. The study also investigates the potential of a diffuser design to analyze the maximum exhaust flow.

The improvement in efficiencies is also analyzed and it proves that improving the exhaust flow does not lead to the expected improvement in efficiency. The findings demonstrate that while certain geometric changes can enhance exhaust flow, each modification presents unique challenges that must be carefully considered.

5. Introduction

In today's world with the rise in battery electric vehicles, it may seem misguided to improve the internal combustion engine (ICE). But there are still many applications that rely on ICE, especially for heavy-duty applications ICE remains the predominant choice for automotive propulsion due to its power density. As efficiency plays a key role in internal combustion engines, every automobile manufacturer is aiming to reduce the losses and ultimately increase the efficiency. One such focus area is the exhaust port. The exhaust port is a fundamental component in the engine's exhaust system, responsible for channeling the burnt gases from the combustion chamber to the exhaust manifold and, ultimately, out of the vehicle. Efficient exhaust gas flow through the exhaust port can contribute to better fuel economy and reduced emissions. Exhaust gases have a lot of available energy which are not utilized properly. According to [Semlitsch et al., 2015] & [Wang et al., 2015] approximately 40% of the available energy is lost as exhaust gas. Even though, some of the lost energy is recovered by the turbocharger, but there are still energy losses due to many reasons like flow structure, and flow profile.

5.1 Objective

The objective of this thesis is to analyze the flow over the exhaust port in the existing geometry and modify the geometry to increase the flow which can ultimately reduce the pumping losses. This task was carried out using computational fluid dynamics (CFD) simulations in Star CCM+. The task was divided into different subtasks. First is to analyze the existing geometry and modifying mesh and turbulence models to match the test results. Second task is to try to optimize the geometry to improve flow in two ways: using adjoint solver and modifying the geometry manually. And the optimized geometry is run at different valve lifts to analyze the overall improvement in the flow. Finally, the improvement in efficiencies is analyzed to see if the flow improvement correlates to improved efficiencies.

5.2 Limitations

- Valve timing, actuation strategies will not be a part of this thesis.
- Star CCM+ CAD environment was used to make modifications in the geometry.

6. Literature Study

This literature review aims to give an overview of the existing losses in an internal combustion engine (ICE) and how it affects the brake thermal efficiency. Further the flow losses also occur due complex geometry structures. These losses can be visualized & analyzed using computational fluid dynamics (CFD) with Star CCM+ software. CFD uses different turbulence models to predict the flow, and the prediction of the flow varies with respect to the turbulence models. The impact of each turbulence model and the most suitable model based on its application will be discussed.

6.1 Combustion Engine Losses

While ICE is used as the main power source for transportation, it inherently experiences several types of losses that affect their overall efficiency. Understanding these losses is necessary while enhancing the engine design and performance. To achieve future targets set by the European Union of reducing the CO_2 emissions requires modification to the existing powertrain systems to have improved efficiency and fuel consumption which can ultimately lead to reduced emissions. According to [Rai et al., 2018], the energy lost in exhaust gases can be recovered, which helps to improve the effective power by improving fuel economy. There are several ways to recover the losses, one of which is the Exhaust heat recovery system. But even with these systems present the losses are still significantly higher.

From [Heywood, 1988] and [Wang et al., 2021], There are four major losses involved combustion losses, heat losses, pumping losses and frictional losses and these can be expressed in terms of efficiency as combustion efficiency, thermodynamic efficiency, gas exchange efficiency, and mechanical efficiency. Figure 1 shows overview of energy breakup in an internal combustion engine.

- Combustion efficiency defines the heat that can be produced by combustion of a fuel. Combustion losses are caused mainly due to fuel not being burned completely in the combustion chamber leading to potential energy loss. Combustion losses was a main concern for spark ignited engines in the early stages of the combustion engine development, but with advanced fuel injection systems and better combustion techniques the combustion losses have rapidly reduced and became very negligible (less than 0.05%). See figure 1 and 2.

- Thermodynamic efficiency defines the conversion of heat into useful work, this is where the majority of losses occur as heat transfer and exhaust heat losses. Heat transfer losses are the energy lost as heat transferred to the cylinder walls, piston and cylinder head which reduces the amount of energy available for doing useful work. Exhaust heat losses are the energy and efficiency lost due to the combustion gases during the exhaust stroke, these carry away a considerable amount of thermal energy that could be used for propulsion. See figure 1, 2 and 3.

- Gas exchange efficiency indicates the ability of combusted gases to be pushed out during exhaust stroke and bring in fresh air into the combustion chamber. This refers to pumping work. Pumping work can be either positive (gain) or negative (loss). Negative pumping work or pumping losses refer to the energy used to overcome the resistance produced during the intake and exhaust process, losses occur when the air needs to move in and out of the combustion chamber, which affects the gas exchange efficiency. During exhaust stroke, when the exhaust gases are pushed through the port and manifold, some resistance occurs, and this resistance leads to pumping

losses. The net power is the useful power available after these losses. See figure 1, 2 and 3.

- Finally Mechanical efficiency describes how much power is converted to the final useful power or brake work. Friction losses express the energy lost as friction to mechanical parts like bearings, valve-train, piston rings and piston cylinder interaction which causes roughly half of the frictional losses. See figure 1, 2 and 3.
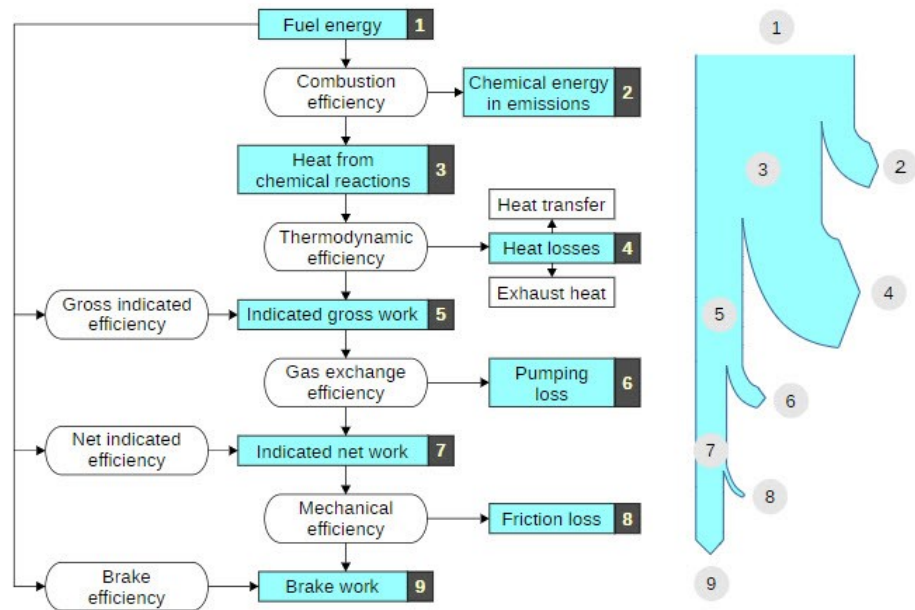
Figure 1 Sankey diagram of efficiency in combustion engine [Majewski and Jääskeläinen, 2023]
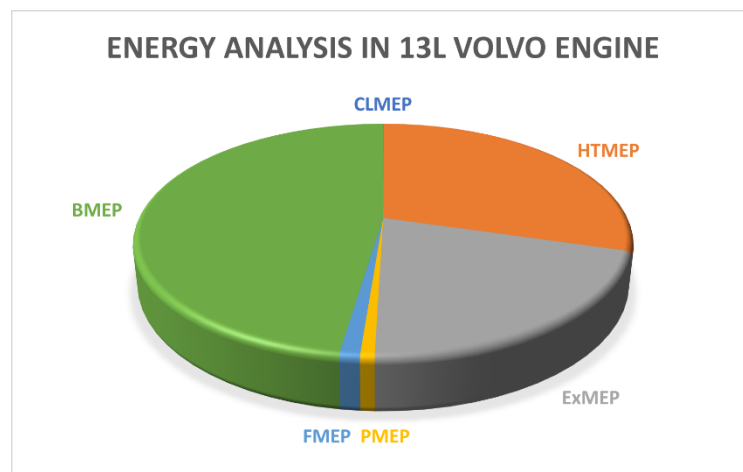
Figure 2 Energy available after losses in a 13L Volvo Engine in the best efficiency point.
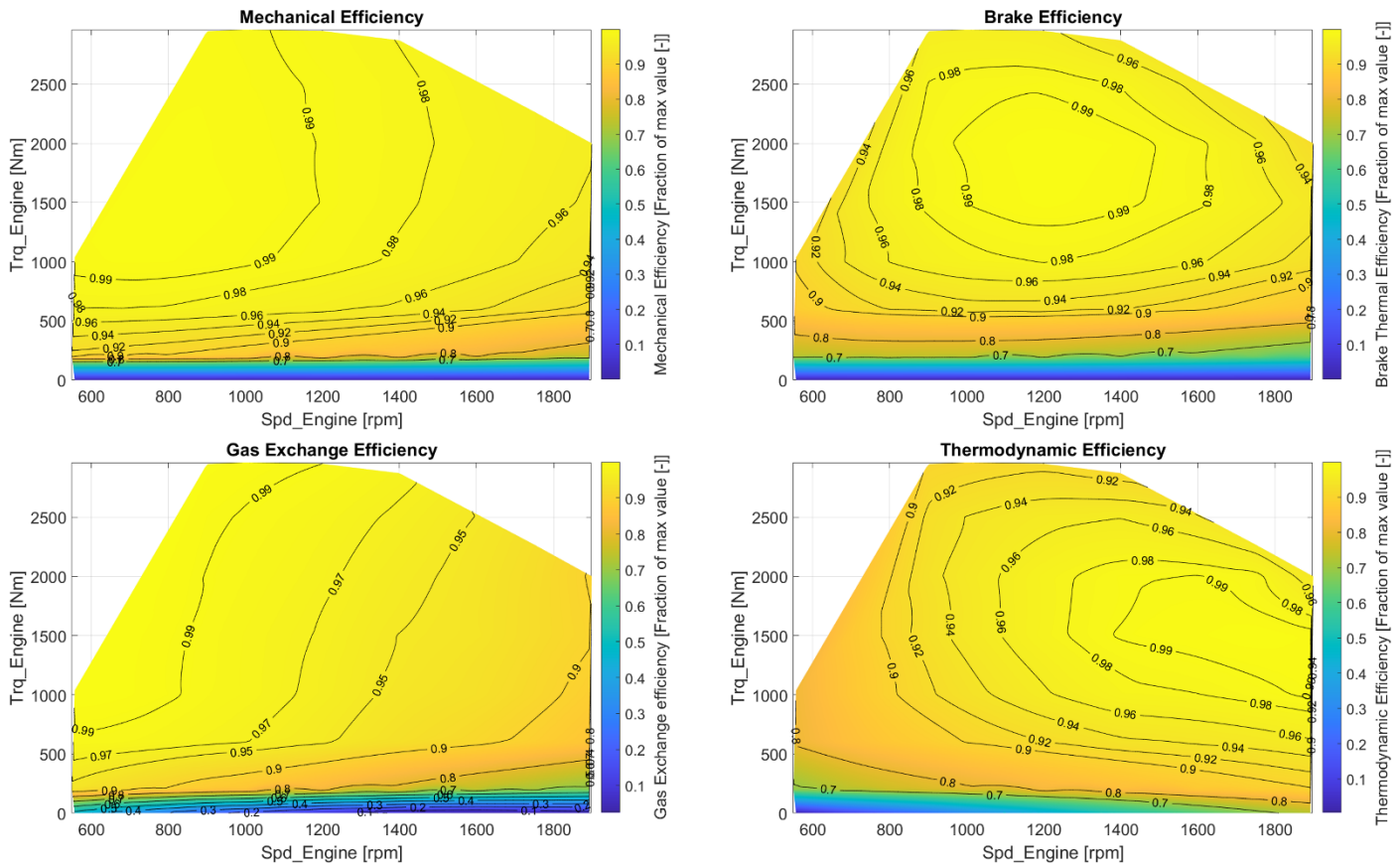
Figure 3 Efficiencies as a fraction of maximum value plotted against speed and torque.

Figure 3 shows the efficiencies of 13L Volvo engine. Brake efficiency is the highest at a medium load point, but it might not be the best operating point. It can also be found that the gas exchange efficiency is highest at lower engine speeds because increased time for intake and exhaust process to occur which allows better scavenging. However, at lower engine speeds other efficiencies drop causing losses to increase. To have a better brake efficiency some sacrifices in terms of losses must be done.

Studies from [Wang et al.,2018] and [Gülmez and Özmen, 2021] state that improving exhaust flow can effectively reduce back pressure, improve volumetric efficiency by facilitating more effective scavenging and enhanced combustion due to improved flow and effective scavenging. With this reduced back pressure due to improved exhaust flow, BSFC and volumetric efficiency can be reduced which can improve the overall efficiency of the engine.

6.2 Exhaust Flow

6.2.1 Flow Losses

Even though a turbocharger helps recover the energy lost during exhaust gas exchange, there are losses occurring in the exhaust port as well due to dissipation and recirculation causing a pressure drop. There are several losses such as friction drag loss caused by viscosity, separation loss caused by centrifugal force which generates vortex and secondary flow losses caused by bending in the exhaust ports due to centrifugal force creating low-pressure zones according to [Xu et al., 2022]. Losses also occur due to variations in the flow path due to cross-section changes like narrowing

(contraction) or expansion of a path. But all of this finally leads to increased pumping losses.

6.2.2 Coefficient of Discharge (CD)

CD is a dimensionless number used to analyze the efficiency of a fluid flow system in complex geometries obtained through tests from flow benches. It is represented as the actual flow rate (measured from CFD simulations or through test bench setup) over the ideal flow rate (calculated using ideal assumptions) or it can also be calculated using effective area and reference area seen in equation 2, from [Heywood, 1988], a flow through a poppet valve is described by using the CD which can be calculated by using equation 1.

$$C_D = \frac{\dot{m}_{CFD}}{\dot{m}_{theoretical}} \tag{1}$$

$$C_D = \frac{A_{effective}}{A_{reference}} \tag{2}$$

$$C_D = \frac{\dot{m}_{CFD}\sqrt{RT_0}}{A_R P_0} \frac{P_T^{\frac{1}{\gamma}}}{P_0} \left[\frac{2\gamma}{\gamma-1} \left[1 - \frac{P_T}{P_0}^{\gamma-\frac{1}{\gamma}} \right] \right]^{\frac{1}{2}} \tag{3}$$

where R is the gas constant, γ is the specific heat ratio, m_{CFD} is the mass flow obtained through CFD simulations, A_R is the reference area, T_0 is cylinder temperature, P_0 is absolute total pressure in cylinder and P_T is absolute pressure at the outlet.

The corrected mass flow is used to compare the results since this shows the mass flow adjusted with reference temperature in cylinder (T_0) and absolute total pressure in cylinder (P_0).

$$m_{corrected} = \frac{m_{actual}\sqrt{T}}{P_0} \tag{4}$$

6.2.3 Valve and Port Geometry Effects on Flow

Port and valve geometry play a vital role in the performance and efficiency of ICE. A well-designed exhaust port can aid in reducing the residual gas fraction inside the cylinder. [Xu et al., 2019] analyzed the impact of port neck area, port outlet area, and port inlet area on flow. Their studies indicate that poorly designed exhaust systems can lead to inefficient flow, increasing exhaust resistance and reducing the gas exchange efficiency. The research shows that flow improves with a smaller port inlet area allowing it to expand gradually along the path to the outlet, and similarly, flow increases with an increased area ratio between the port neck area and inlet of the port. This suggests that the port inlet area should be smaller compared to the port outlet area, aligning with Bernoulli's principle.

The primary design factors influencing the escape of burnt gases through the ports are the cross-sectional area and the smooth curvature radius, which help prevent flow separation and recirculation. [Singh et al., 2019]

found that reducing pumping losses by decreasing work done in pushing the exhaust gas can enhance exhaust gas flow, achievable by optimizing port geometry through variations in the port area above the throat area, smoother curvature, or specific valve angles.

Studies from [Hires and Pochmara, 1976] show that the shape of the exhaust port has its effect on the heat losses through exhaust port. Six different types of port geometry were analyzed at three exhaust mass flow rates and among that longer exhaust port tend to have more heat losses at higher mass flow rates whereas port with reduced flow area above the throat has comparatively lower heat losses at the same mass flow rates.

[Xu et al., 2022] studied the effects of valve recess, valve seat diameter, port profile on energy loss trends, and separation losses. The radius of bends in the port significantly impacts the separation region; a higher radius in the lower bend or a lower radius in the upper bend reduces the separation region. Additionally, energy loss is inversely proportional to the discharge coefficient, indicating that optimizing these geometric factors can lead to more efficient exhaust gas flow.

6.2.4   Venturi Theory

The venturi effect refers to an increase in velocity and a decrease in pressure that a fluid experiences while going through a constriction. Figure 4 shows a typical venturi tube. To understand the venturi effect, Bernoulli's principle is used to establish the relationship between pressure and velocity if a fluid. Bernoulli's principle is based on conservation of energy which states that in a steady and streamlined flow the sum of all energy (kinetic, potential, and internal energy) should remain constant. This means that when the kinetic energy increases the potential energy must decrease. The Bernoulli's principle can be expressed as shown in equation 5.

$$\frac{v^2}{2} + gz + \frac{p}{\rho} = constant \tag{5}$$

Where v is the velocity of fluid, g is the acceleration due to gravity, z is the elevation, p is the pressure, and ρ is the density of fluid.
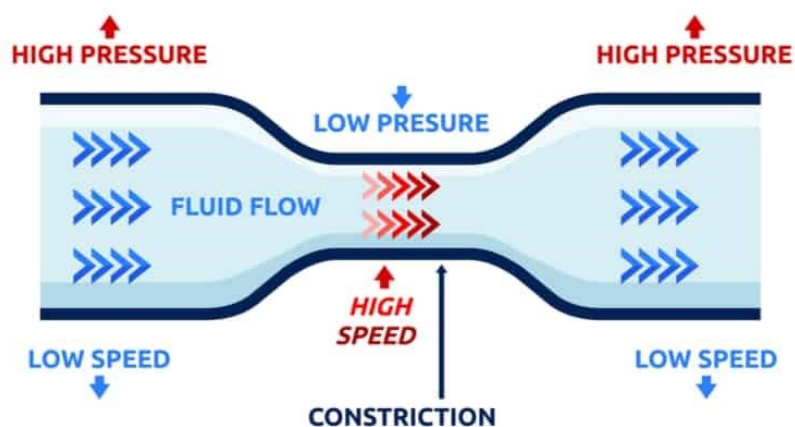
Figure 4 Venturi tube describing the pressure and speed of flow through constriction [Cadence CFD, 2022].

Equation 6 give an understanding of how mass flow(m) varies with respect to velocity(v) and effective area(A).

$$m = \rho A v \qquad (6)$$

6.2.5 Diffuser Theory

Diffuser's purpose is to reduce the velocity of the flow which results in increased pressure [Dixon and Hall, 2013]. Diffuser is also like a venturi, since it follows Bernoulli's principle but focuses on increasing the pressure by decreasing the velocity with aim of having low losses. A diffuser can be visualized as shown in figure 5.
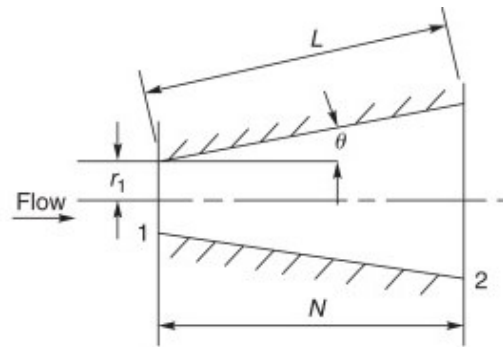
Figure 5 A typical diffuser design where 1 is inlet and 2 is outlet [Dixon and Hall, 2013].

Equation 7 can be used to design a diffuser where A_1 is the inlet area, A_2 is the outlet area, N is the distance from inlet to outlet, r_1 is the inlet radius and θ is the angle of expansion measured from inlet.

$$A_R = \frac{A_2}{A_1} = [1 + \frac{N}{r_1}\tan\theta]^2 \qquad (7)$$

While designing a diffuser the expansion angle θ is important since the flow starts to separate from the diffuser walls. Therefore, the optimum angle for a diffuser is about 5 to 7 degrees which gives an optimum diffusion rate.

An annular diffuser is when there is a conical surface in the middle making the flow path more restricted. This is the case when there is a port and a valve inside. The sectional view of an annular diffuser can be seen in figure 6.
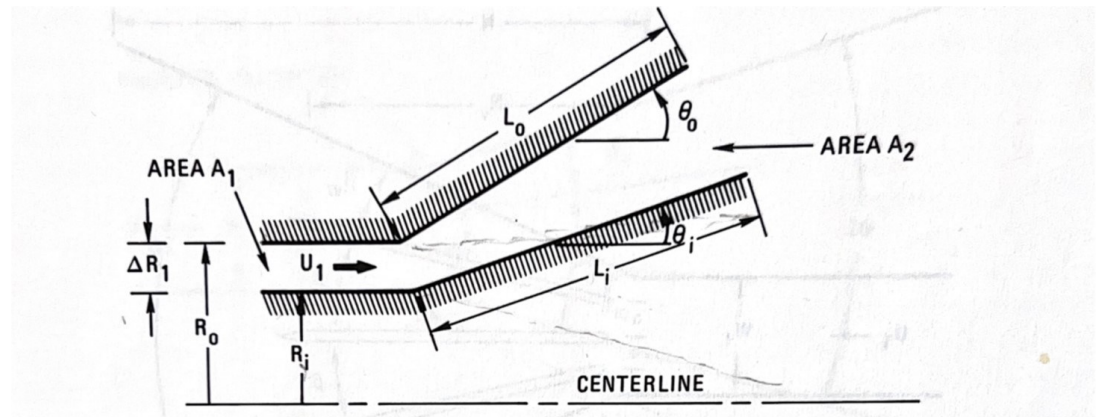
Figure 6 Cross section of an annular diffuser which is rotationally symmetric (Blevins, 1984).

6.2.6 Losses with contraction and expansion

From the studies of [Wang, 2013], a contraction and an expansion in a path have significant effects on the flow behavior with respect to velocity and pressure. When a flow approaches a contraction, the flow velocity increases causing the pressure to decrease. Eventually, the flow paths expand again which results in increased pressure and decreased velocity.

Contraction: From [Holmberg et al., 2017], [Wang, 2013] and [Boger and Walters,1993], fluid flow through contraction increases the velocity and a decrease in static pressure is observed based on Bernoulli's principle. When there are sudden contractions there can be some recirculation zone appearing upstream of the throat section (or the narrowest section), but during contraction, the main recirculation zones can be found at the entry of the throat near the walls which can be seen in the upper part of figure 7. These cause dissipation in turbulence which increases the losses in energy. Energy losses are proportional to velocity flow.

Expansion: When the area expands or fluid flows from a smaller area to a larger area pressure increases and velocity decreases. This is what the diffuser theory also states. Due to this expansion, some recirculating flow appears downstream of the expansion which can be seen in the lower part of figure 7. It is these recirculation zones that contribute to energy losses and these energy losses are proportional to the flow velocity.
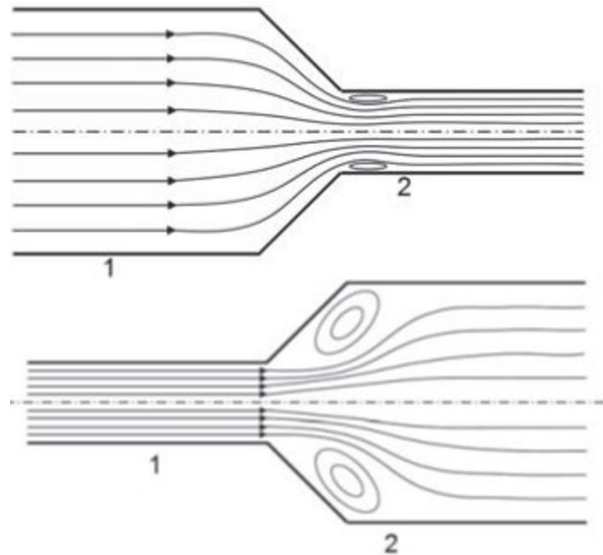
Figure 7 The upper figure shows a contraction path, and the bottom figure shows an expanding path. [Wang, 2013]

6.3 Turbulence Models for CFD

Turbulence models are mathematical expressions employed in computational fluid dynamics (CFD) to mimic the impact of turbulence in fluid movements. Turbulence in fluid motion is characterized by chaotic and random fluctuations commonly found in numerous engineering situations. It is essential to model turbulence as simulating all turbulent scales directly would demand vast computational resources. Instead, turbulence models offer a convenient method for efficiently simulating these effects. From the studies of [Wang, 2013] and [Wang et al., 2015] there are two main classifications: models that use RANS (Reynolds-Averaged Navier Stokes) and scale resolving models that use LES (Large Eddy Simulation) and DES (Detached Eddy Simulation). LES explicitly solves the larger turbulent scales and models the smaller scales whereas DES is a hybrid LES-RANS approach that resolves turbulent structures and covers the wall boundary by a RANS model. It requires solving Navier-Stokes equations with a filter that eliminates small turbulent scales. LES requires more computational power than RANS and DES, however, it provides a more detailed representation of turbulence, especially in flows with large-scale structures. On the other hand, the RANS model uses time-averaged equations to quantify the flow quantities to solve the fluctuating components. There are two common turbulence models used for CFD which are the k-ε and k-ω. The RANS model is more suited for ICE since it requires less computational power in comparison to other models and due to this reason, it has become the industry standard for most flow simulations.

6.4 Summary

After analysis of different losses, it is evident from the above literature review that losses due to exhaust flow can be reduced. Most of the losses can be reduced by making some changes to the geometry which will ultimately reduce the separation of flow and is able to escape from the combustion chamber faster to have reduced pumping losses. The flow behavior in the exhaust port can be analyzed using CFD which uses turbulence models to capture flows accurately. From the study it is found that RANS models are the most suited turbulence models for the simulation of exhaust port flow as it can accurately capture the flow accurately and as it has become industry standard to use RANS for flow simulations. Venturi theory provides that after a contracting path the expanding

flow must be more controlled to avoid losses and faster diffusion. This thesis will use these concepts to analyze the possibilities to improve exhaust flow and reduced pumping losses.

7. Method

This work was carried out in Star CCM+ v.2306. Simcenter Star CCM+ CFD software was used for this thesis. It is a Multiphysics computational fluid dynamics simulation software which allows for modelling various types of flows, heat transfers, turbulence, aero-acoustics, and much more complex flow behavior. First, the geometry is set by extracting the CAD model, and then physics models are chosen based on the type of simulation (steady or unsteady, gas or liquid, turbulence model) and then geometry is assigned to regions where the boundary conditions are set. Mesh is created by defining different parameters selected like mesh type, prism layers, base size, and surface proximity. The conditions applied to the exhaust port geometry are mentioned in the upcoming sections. The methodology is shown in figure 8.
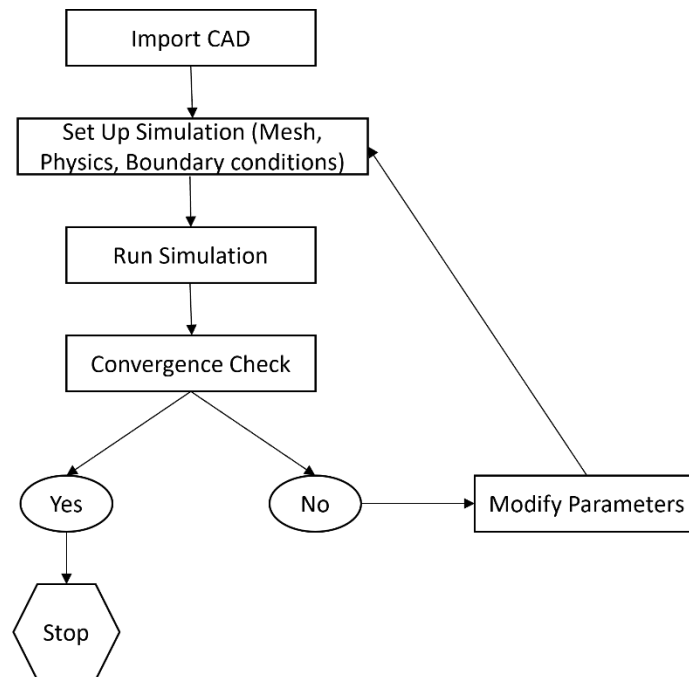
Figure 8 Procedure for solution setup.

Steady state simulations were performed. This work consisted of analyzing the flow in the existing geometry and optimizing the geometry to achieve better flow. The flow was analyzed for valve lifts 1-14mm. So, to optimize the flow a single valve lift, 5mm lift was chosen to achieve the desired flow. Later, if the desired flow is achieved, the new geometry will also be simulated for 1-14mm valve lifts to see how it performs.

7.1 Model

The model contains cylinder liner, exhaust port and valves from a 13L diesel engine which can be seen in figure 9. Star CCM+ has been used to analyze the geometry.
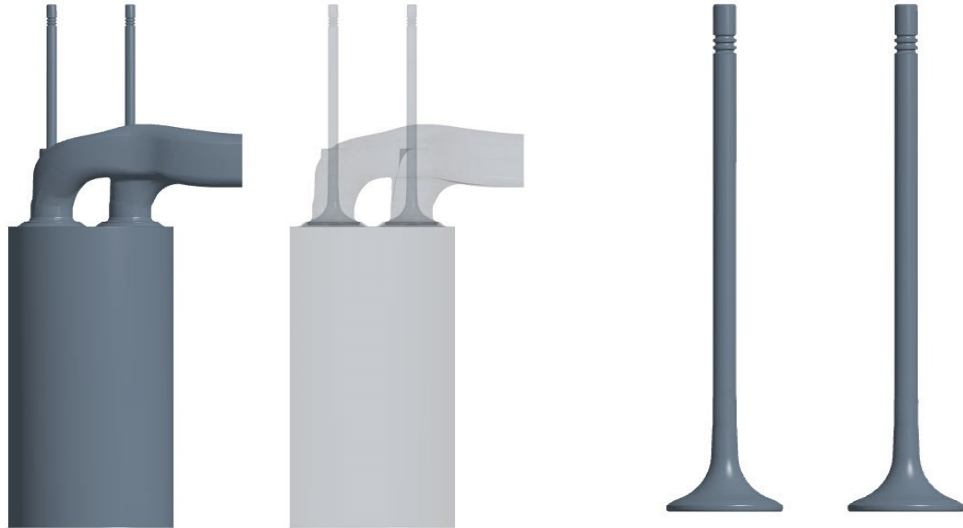
Figure 9 Base Geometry with a transparent view of section at the left side of the figure and the exhaust valve in the right side of figure

7.2 Mesh

Mesh generation is ideal for attaining numerical solutions to governing differential equations. The geometry is divided into a finite number of small elements or cells, forming a computational grid. The mesh accurately represents the geometry to be simulated, ensuring the simulation can capture complex and intricate details of the flow field around complex structures. It is important to have an accurate mesh to have a well resolved solution, with finer mesh the computational cost increases. There are many mesh settings available in Star CCM+ and the mesh chosen for this thesis is a polyhedral mesh of base size 2mm along with prism layer mesh with 10 prism layers, 1.5 stretching and, thickness of 50% with respect to base mesh size. Along with this surface controls were used to specify wake refinement with a range of 15mm and spread angle of 30 deg to have a refined mesh near the valves and port inlet. Prism layers are disabled at the inlet and outlet boundaries since there is no wall boundary to resolve. The difference in the mesh before and after wake refinement is applied can be seen in figure 10&11.

Initial Mesh   Sectional view
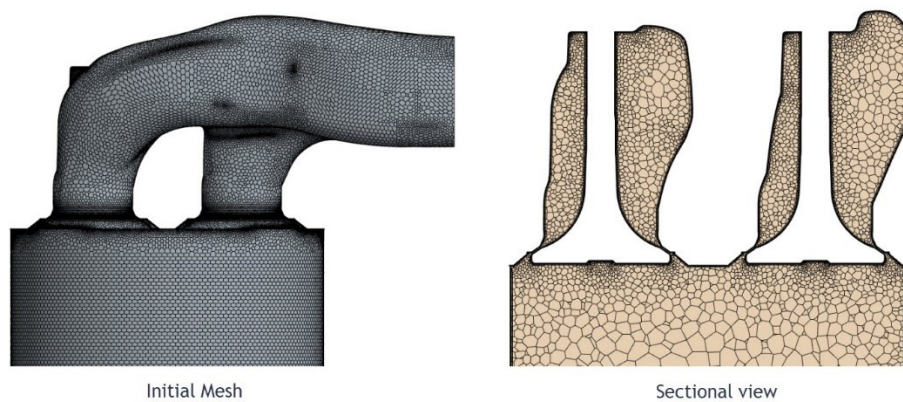
Figure 10 Mesh before refinement

Refined Mesh   Sectional view
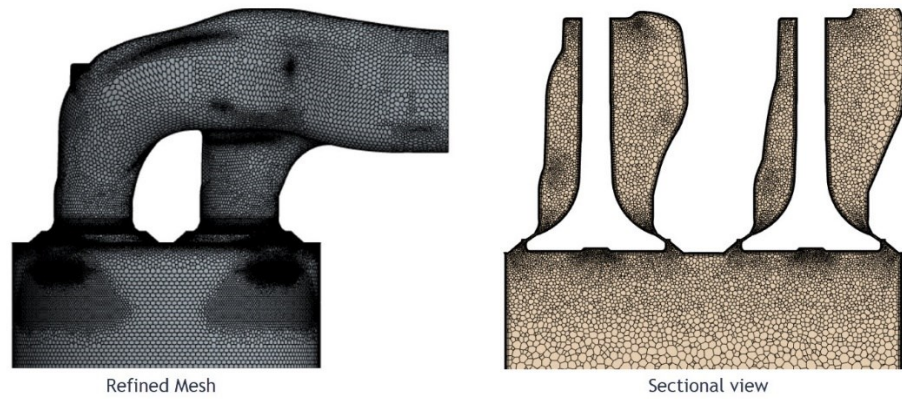
Figure 11 Mesh after refinement

7.3 Physics and Solvers

The flow was modeled as steady state. First K-epsilon turbulence model was used, but with this model the flow was not converging at several valve lifts between 4 to 10mm even with 2000 iterations for each lift which can be seen in figure 12, later using K-omega turbulence model with 10000 iterations showed good convergence (reduced fluctuations) which can be seen in figure 13. Coupled energy and flow solver were used and the solver was set with convergence accelerator and an automatic CFL control method.
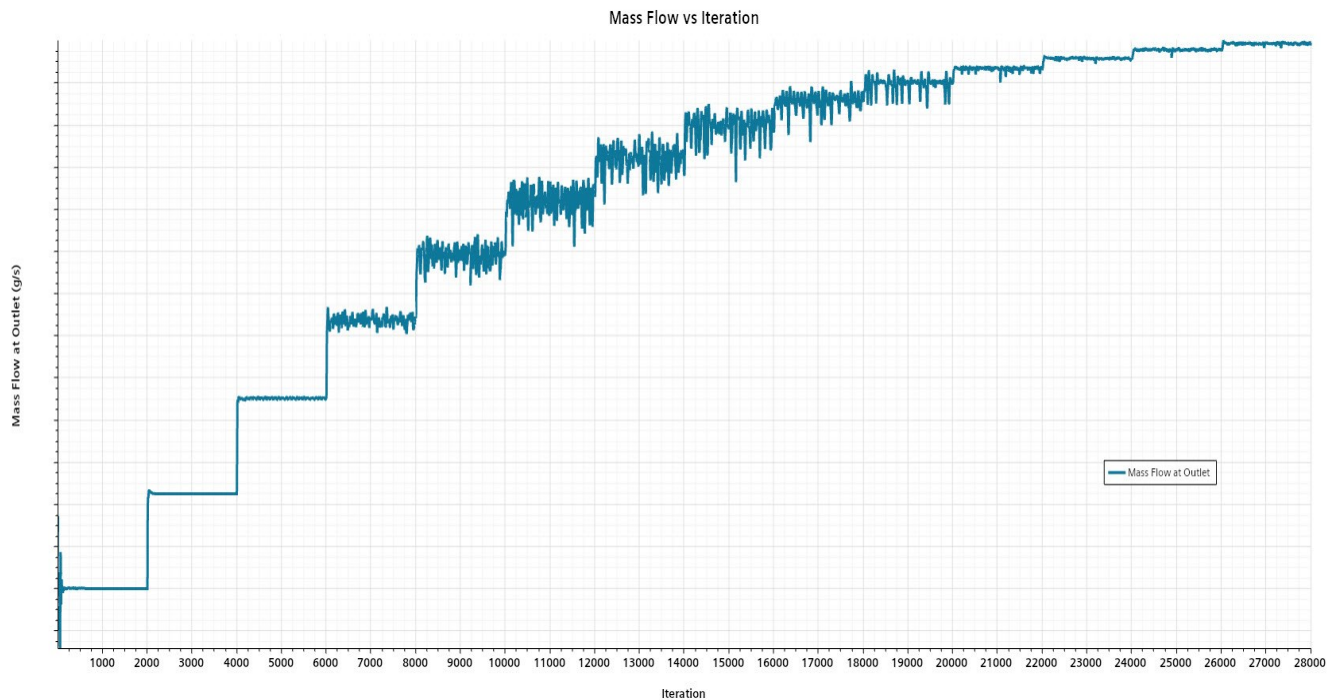
Figure 12 Mass flow monitored with respect to iteration upper plot showing fluctuation in mass flow.
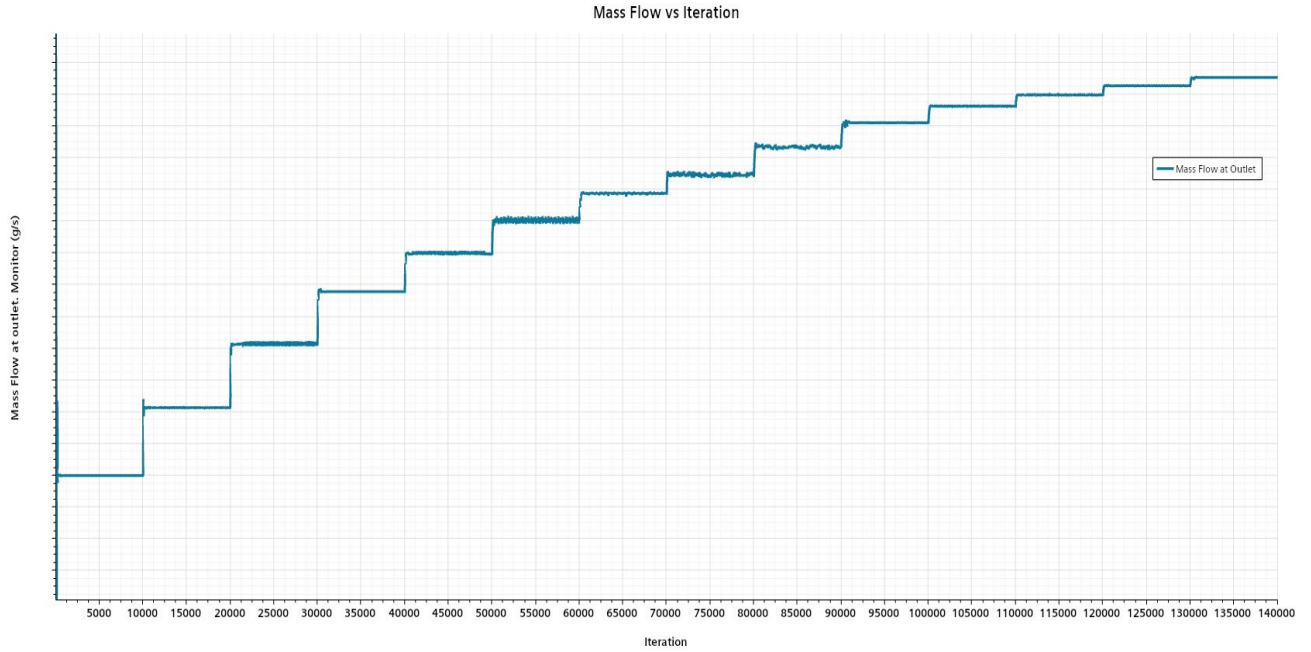
Figure 13 Mass flow monitored with respect to iteration shows little to no fluctuations in mass flow compared to figure 11.
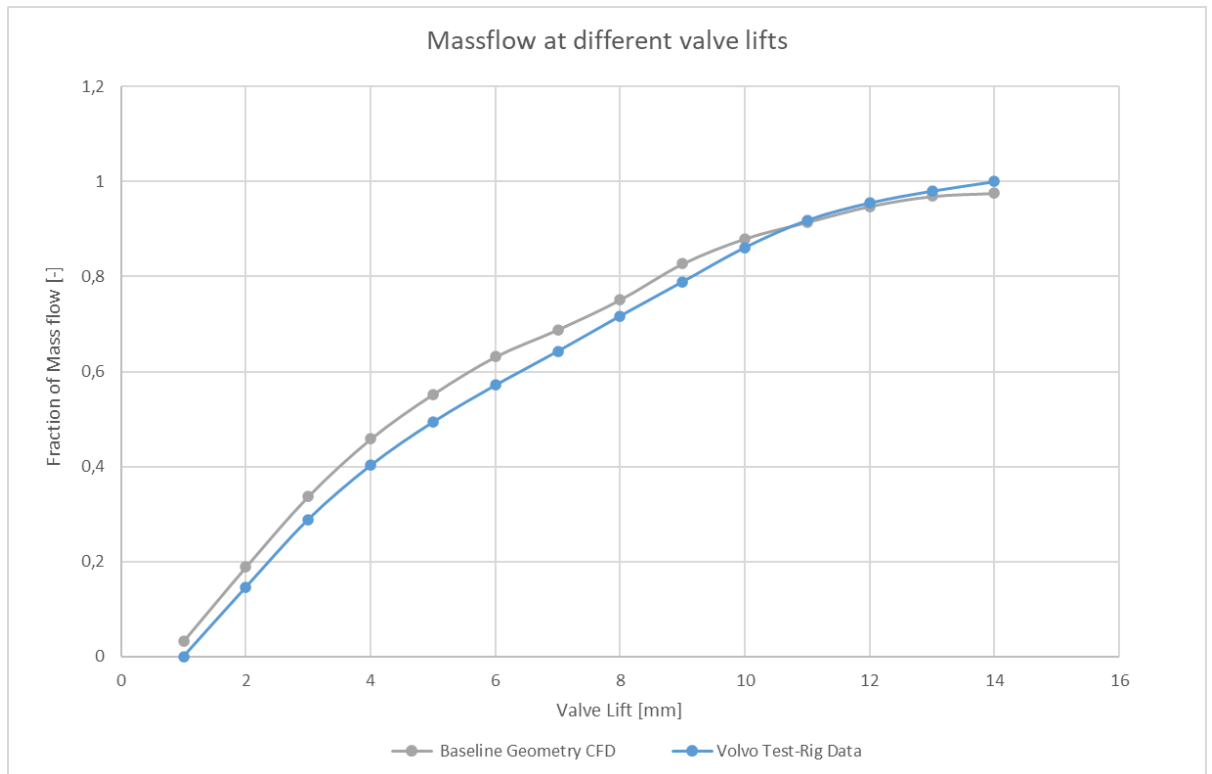
Figure 14 Mass flow as function of valve lift. Test result compared to simulation results. The mass flow is expressed as fraction of the maximum flow in the flow test.

7.4 Boundary Conditions

Boundary conditions are essential for defining how the fluid interacts with the environment. They are critical for ensuring that simulations are realistic and physically accurate. Where there exist inflow and outflow boundaries within the flow domain. For this simulation, a stagnation inlet and pressure outlet are used.

Stagnation inlet had a total pressure of 106.3 kPa and the outlet pressure was set to 101.3 kPa. The pressure difference is kept 5 kPa, since this was followed in rig tests carried out, it would be easy to compare the results of the simulation to the actual test to have them accurate enough.

However, these boundary conditions do not correlate to real engine boundary conditions since it is much higher than this. In real engines the pressure difference would vary between 5 to 10 bar (500 to 1000 kPa). In simulations for easier computation and better analysis lower values are used to capture the characteristics.
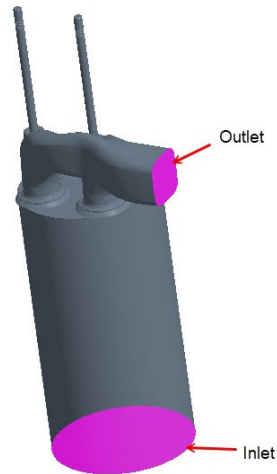
Figure 15 Regions where inlet and outlet boundary conditions are applied.

7.5 Area vs distance

In this chapter a rotationally symmetric exhaust port is considered to analyze the fundamental effect of how to diffuse the flow. To evaluate the area vs distance a mathematical expression is needed that works for the full exhaust port. The exhaust port is essentially a flow channel with an inner body. The equations for this are trivial for both a channel that is radial and axial. However, in an exhaust port, the flow is not purely radial nor purely axial. For that reason, the equations are rewritten to be universal for both axial flow channel, radial flow channel and mixture thereof, see equation 8 to 10.

$$Radial\ flow\ area = 2\pi dr => \pi d(r_1 + r_2) \tag{8}$$

$$Axial\ flow\ area = \pi(r_2{}^2 - r_1{}^2) = \pi(r_2 - r_1)(r_2 + r_1) => \pi d(r_2 + r_1) \tag{9}$$

$$Effective\ flow\ area = \pi d(r_1 + r_2) \tag{10}$$

Where r1 the radius from the center to the valve surface, r2 is the radius from center to the port surface and d is difference in the radius (r_2-r_1).

7.6 Effective area vs distance

The effective flow area of a port significantly affects the engine's performance. Understanding this is crucial for optimizing exhaust gas flow. Effective flow area impacts measure the capacity of exhaust port to allow exhaust gases to flow out of combustion chamber. The actual shape and dimensions of the exhaust port affects the ease of exhaust gas flow through it. This helps to understand the flow characteristics along the length of exhaust port to identify potential bottlenecks and aids in optimizing the design.

The effective flow area is dependent of how the area increase is. The outlet and inlet area are fixed due to design restrictions. The inlet area is at the valve seat and the outlet area is the same area as the exhaust manifold inlet area. The outlet area to inlet area ratio constant. When the effective flow area increase needs to be in a smaller value the length of port is increased and vice versa. In figure 16 with an expansion angle of 6.5 degrees, the plot in figure 17 the left side plot shows the effective flow area vs distance from valve seat when optimized for 10mm lift while evaluating at 5mm lift, and the plot towards right shows how to minimum effective flow area varies at valve lifts from 1-14mm when optimized at 10mm lift. In figure 16 with an angle of expansion of 5 degrees in the right figure, it is like the previous case but the opposite which means the plot in figure 18 shows effective flow area when optimized for 5mm while evaluating 10mm lift. It can be observed that the minimum effective flow area drops at higher valve lifts in figure 18 compared to figure 17.

Figure 19 shows the how optimizing at different lift changes the effective flow area. It shows that optimizing at 5mm lift the effective flow area is worse at larger lifts whereas optimizing at 10mm lift affects the effective flow area at smaller lifts. This suggests that a balance between good effective flow area at higher lifts and optimal expansion area for smaller lifts is required for good flow performance characteristics.
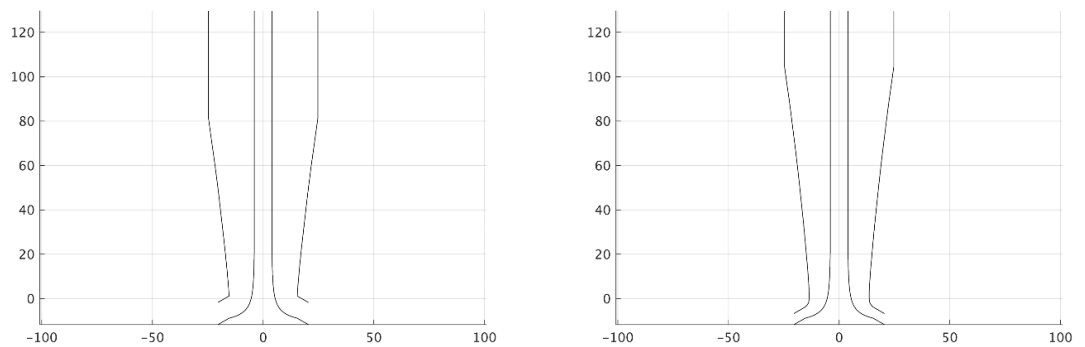
Figure 16 The left figure shows port with an angle of 6.5 degrees when optimized for 10mm; The right figure shows a port with an angle of 5 degrees and optimized for 5mm.
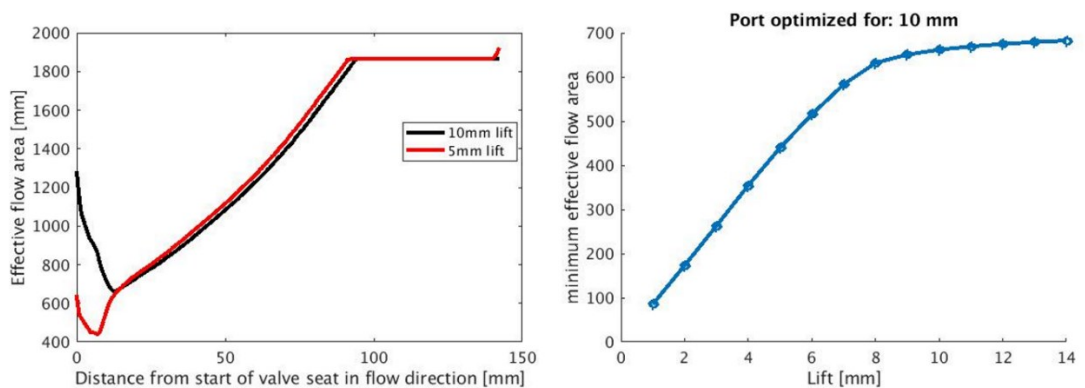
Figure 17 The left figure shows the effective flow area vs distance when optimized for 10mm lift while evaluating at 5mm lift. The right figure shows the minimum effective flow area vs lift when optimized for 10mm.

.
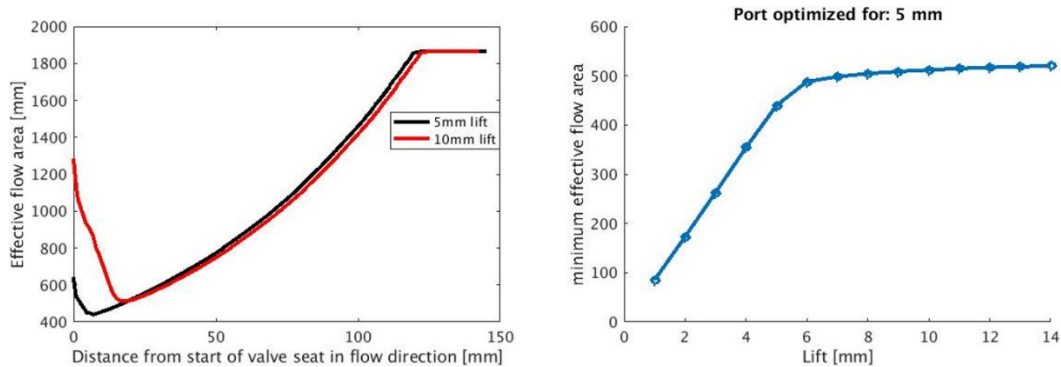
Figure 18 The left figure shows the effective flow area vs distance when optimized for 5mm lift while evaluating at 10mm lift. The right figure shows the minimum effective flow area vs lift when optimized for 5mm.
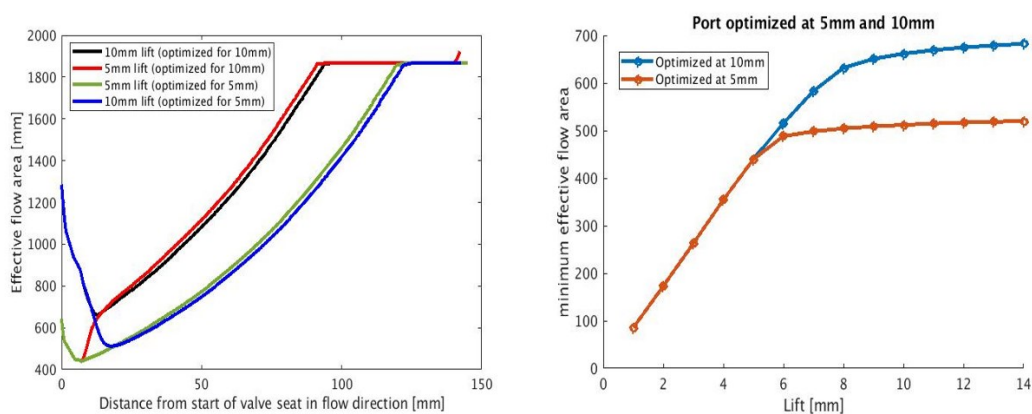
Figure 19 This figure is a combination of both figure 17 and 18.

7.7 Diffuser

As seen in the literature review the main aim of a diffusers is to decelerate the fluid flow while simultaneously increasing its pressure. Since this deceleration of fluid leads to decrease in mass flow as well the expansion of diffuser must be more subtle. The main aim of the diffuser is to find the upper limit of mass flow rate. The narrowest region in this case is the region between the valve seat and the valve itself which can be seen in figure 20 indicated with red line.
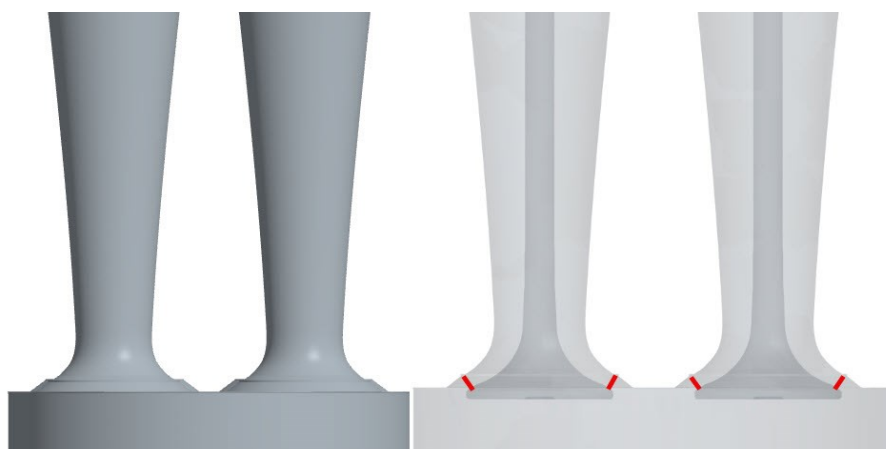
Figure 20 Diffuser design where the red line indicates the narrowest region.

25

7.8 Optimization techniques

Optimization is a process to find the best solution to achieve best performance under some conditions and constraints. This is done by adjusting parameters to achieve the objective. In this case optimization is done to achieve improved flow in the exhaust port. The modifications of parameters, here it is the port geometry shape itself, are done downstream of the valve seats. There are two methods through which optimization can be done adjoint solver and parameter optimization [Hopf, 2022].

7.8.1 Adjoint Solver

Adjoint solver is an optimization method in Star CCM+ used to predict the influence of many design parameters and physical inputs based on the required target. It works based on a cost function coupled to the adjoint solver and surface sensitivity which then deforms the mesh/geometry to obtain a primal solution. This method is effective where the objective is to either minimize or maximize a performance parameter like pressure loss or drag. This method works based on mass flow inlet and pressure outlet boundary condition where the aim is to reduce the pressure drop. The adjoint solver was tried with a target mass flow at the inlet, but the resulting geometry changes were strange, and no solutions were found with the limited time, due to which this optimization method was abandoned.

7.8.2 Parameter Optimization

Parameter optimization making changes to parameters like diameter, angle and these changes are made to the base geometry to analyze the effect of these modifications in mass flow. Several different cases were tried with modifying in different types. Some cases gave a good improvement in the flow whereas some cases are not practically possible to do but were just evaluated in CFD.

8. Base Geometry

After understanding the best parameters for mesh, solver and physics, a full sweep at all valve lifts was performed to verify with the test results. Figure 20 shows flow in terms of velocity at different lifts. The color scheme represents the velocity of flow at that region, where blue represent the lowest velocity and red represents the highest velocity. The plot in figure 14 shows mass flow as a fraction of maximum value at each valve lifts and approximately 5-10% difference in the results were found on an average. This means that the optimized flow should be 5-10% higher than the target flow. At lower valve lifts a lot of recirculation zones appear.
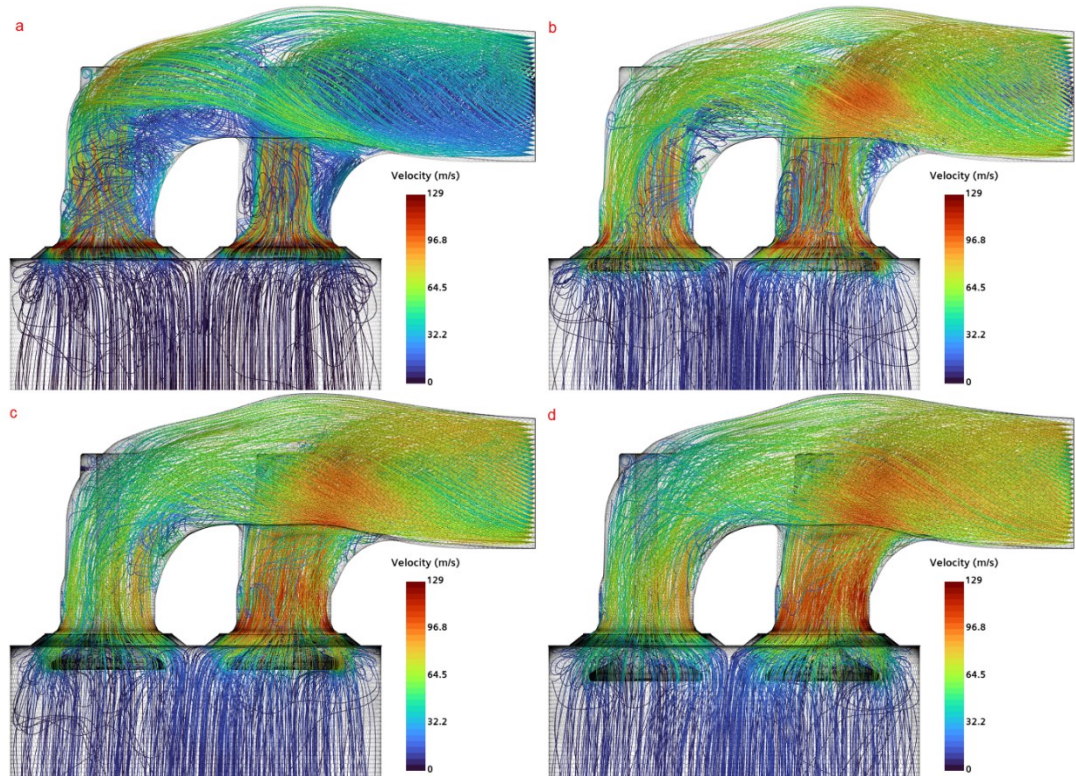
Figure 21 Flow over different valve lifts a) 2mm, b) 6mm, c) 10mm, d) 14mm.

9. Results

9.1 Parameter Optimization

9.1.1 Case 1:

In this case the port is moved close to the cylinder head such that the valve face is exactly in line with the cylinder head at fully closed condition. This case was a random trial to see if moving the port down could reduce the recirculating flow. This modification can be seen in the figure 22 below where the black arrows indicate the changes made. The flow improved by one percent at some valve lifts which can be seen in the figure 23.
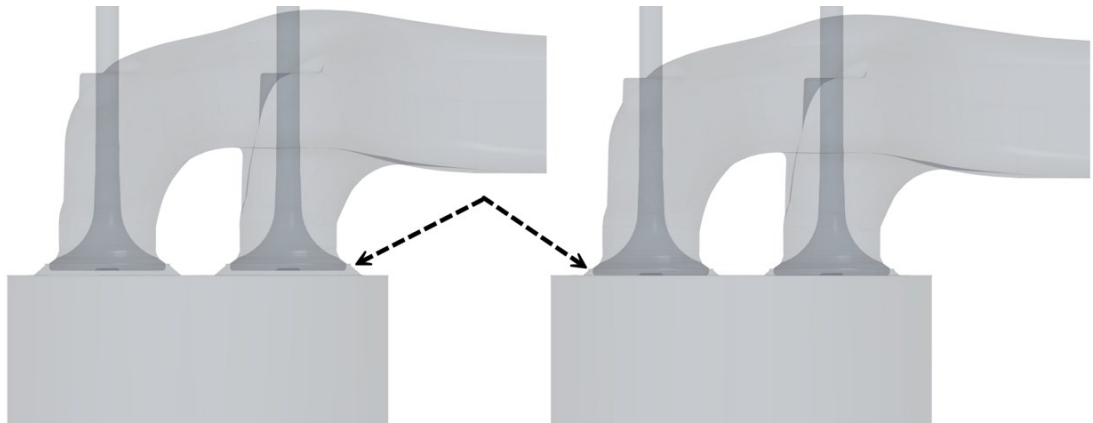
Figure 22 Port moved down to have valve face in line with cylinder head compared to base geometry in left, the changes made are indicated with the black arrows.
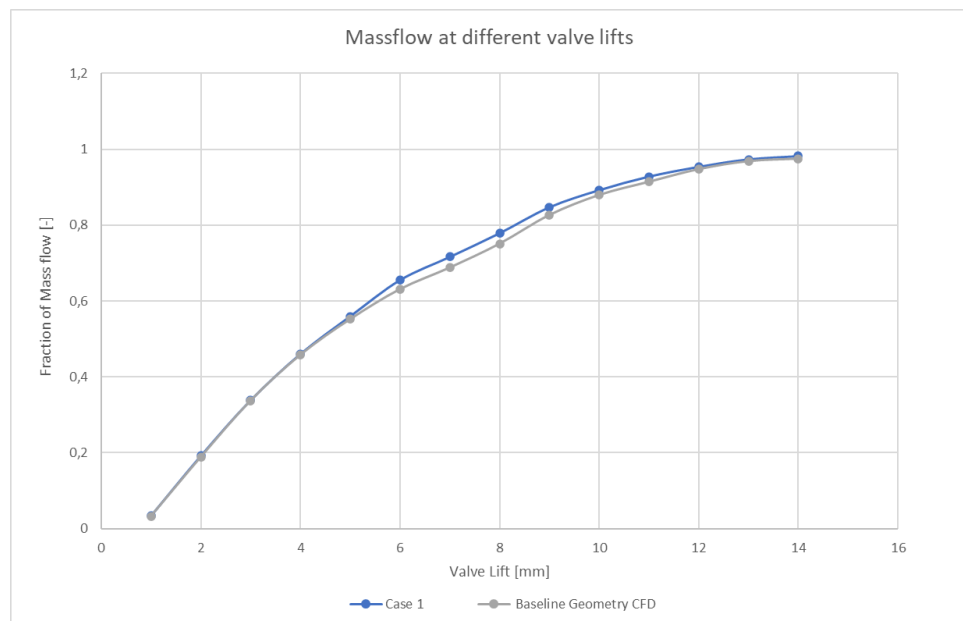
Figure 23 Mass flow as function of valve lift. Valve in line with cylinder head compared to simulation results. The mass flow is expressed as fraction of the maximum flow in the flow test.

9.1.2 Case 2:

In this case the port is directly over the cylinder head. This means the valve seat sits over the cylinder head. The changes made can be seen which is

28

indicated with the black arrow in figure 24. The flow is very similar to the base geometry at most of the valve lifts which can be seen in figure 25.
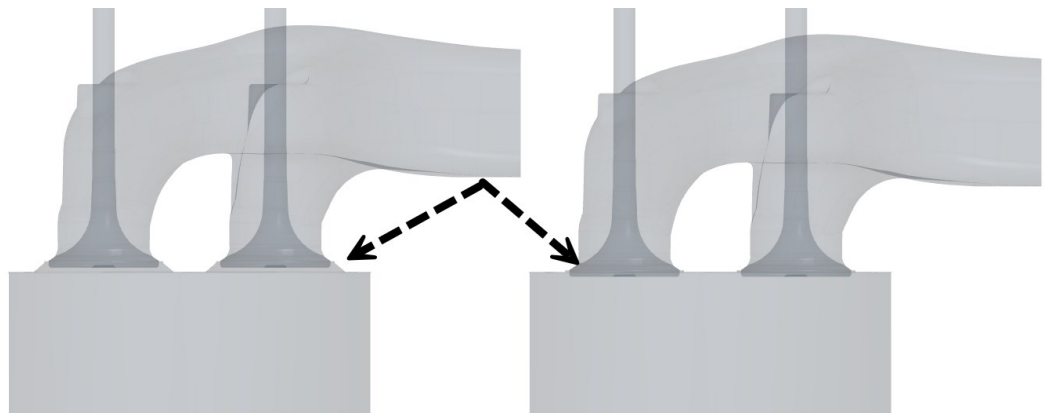
Figure 24 Port moved to the cylinder head compared to base geometry in left, the changes made are indicated with the black arrows.

Figure 25 Mass flow as function of valve lift. Port at firedeck compared to simulation results. The mass flow is expressed as fraction of the maximum flow in the flow test.

9.1.3   Case 3:

From the earlier review on port geometry effects on exhaust flow, it was evident that making changes to the above the port throat area gives an improved flow as well as reduced heat losses as well. To evaluate that modifications are made at the above the throat of exhaust port. Using the 3D CAD environment in Star CCM+ the geometry was changed after the valve seat (keeping everything the same till valve seat). A parameter was used to control how deep the curvature of the port neck should be. This was performed to understand the venturi effect of how a constriction will affect the flow behavior.

The modification was done with different curvatures and had a parameter with value of varying from 1mm to 3mm and was found that it performed well at around 2mm. This means that the radius of the area above the throat is reduced by 2mm which means the port is curved inwards as show in figure 26 where the black arrow indicates the changes.

29

Many values for this modification were tried but out of those only 2mm gave the best results in comparison to that with base geometry.

The modification was done manually to improve the flow at valve lift 5mm. The maximum achievable mass flow improved by about 5.4% higher compared to base geometry. Majority of the losses in flow can be seen in figure 27, where the dark blue region near the curvature shows a zone which contain some recirculating flow.
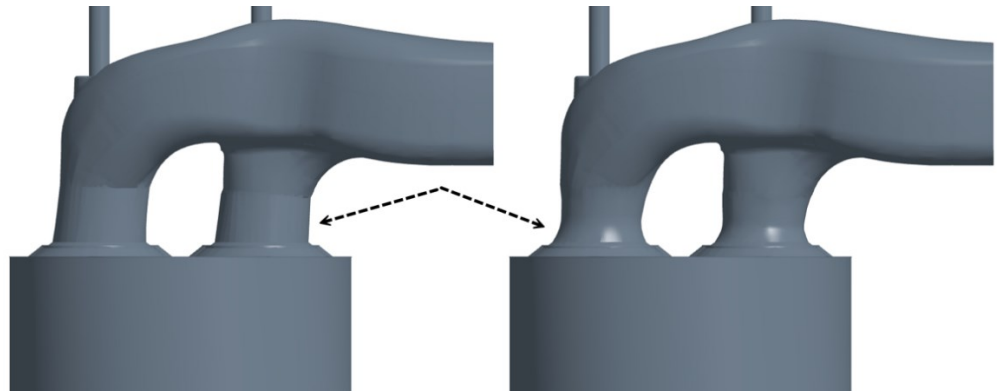
Figure 26 Modified Port throat area in the right compared to base geometry in the left, the changes made are indicated with the black arrows.
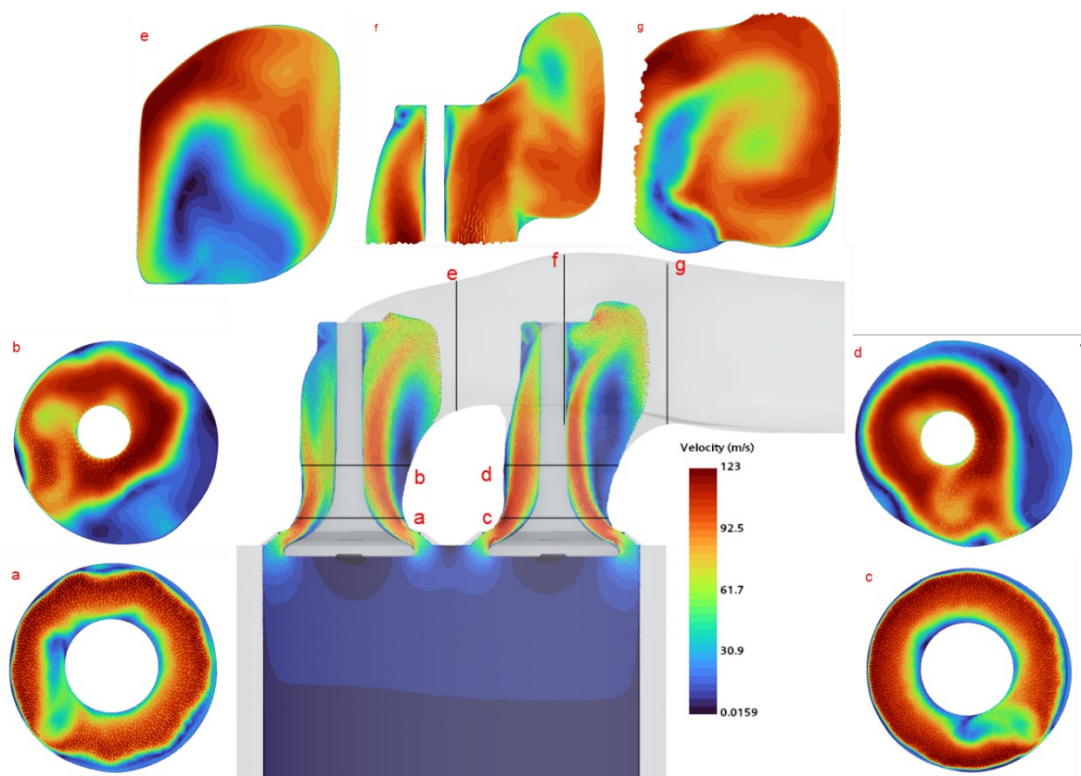
Figure 27 Flow in terms of velocity at different section of the port at 5mm lift with manual modified geometry. All the sections are represented with the same scale values for velocity.

With the above modified geometry, the flow at different lifts can be seen in the figure 28.
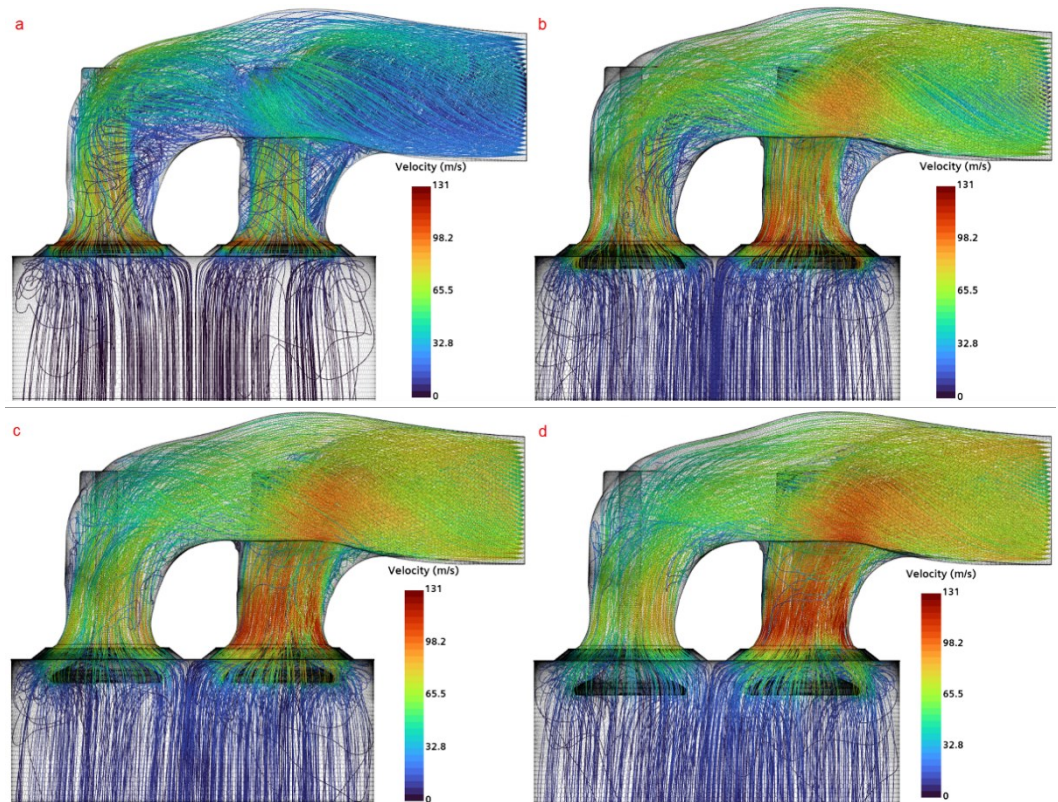
Figure 28 Flow in terms of velocity at different valve lifts a) 2mm, b) 6mm, c) 10mm, d) 14mm.

When compared to the flow with base geometry there are certain region near the curvature just above the port throat, where the recirculating flow has reduced. This is the reason for improved mass flow as well. The plot of flow at lifts 1-14mm can be seen in figure 29, where good improvement can be seen at the intermediate lifts.
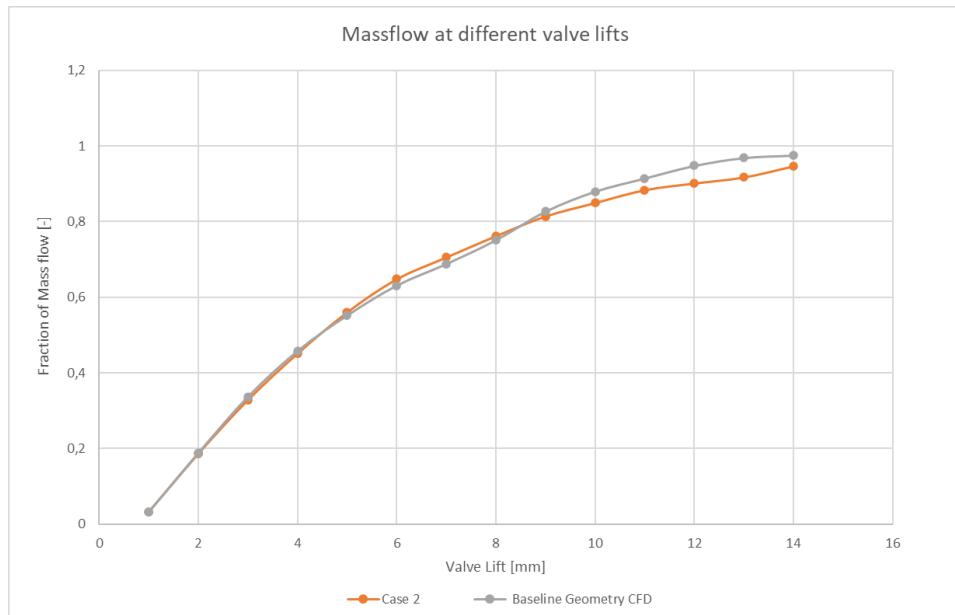

Figure 29 Mass flow as function of valve lift. Modified port neck compared to simulation results. The mass flow is expressed as fraction of the maximum flow in the flow test.

31

Various other manual modifications were tried where the flow improved in comparison to the base geometry but was not the best when compared to the case above.

9.1.4 Case 4:

A small amount of flow separation can be seen in figure 27 near the valve edges. This case was a trial to see if the flow improved when the separating flow can be reduced. In this case the sharp edge at the valves were smoothened to see the effects. The black arrows in figure 30 show the geometry before and after smoothening. This was done using fillet option in 3D CAD environment in Star CCM+. When this was combined with case 3, the flow improved by 6.9 % at valve lift 5 mm due to reduction in flow separation near the valve edge. But this reduces the valve seat area, and this is not the best thing to do since it will reduce the contacting area and reduce the heat dissipation capacity. Flow versus valve lift is shown in figure 31.
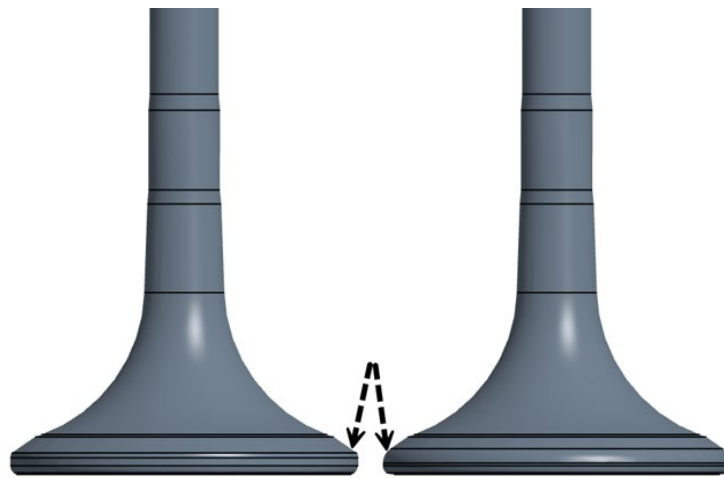
Figure 30 Valve edge smoothened compared to base valve design in the left, the changes made are indicated with the black arrows.
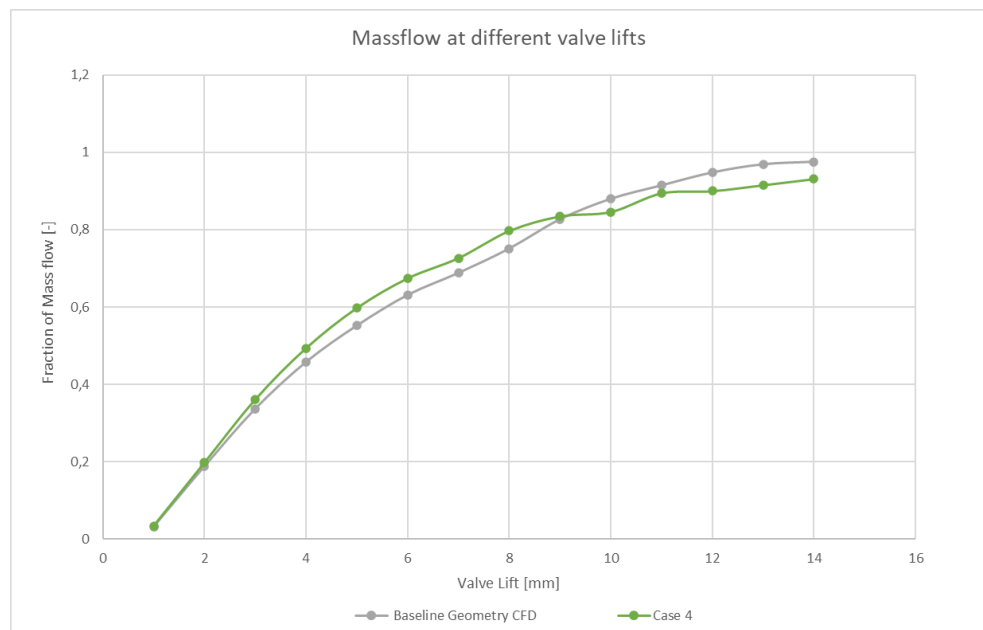
Figure 31 Mass flow as function of valve lift. Valve edge smoothened compared to simulation results. The mass flow is expressed as fraction of the maximum flow in the flow test.

32

9.2 Diffuser

9.2.1 Diffuser Design 1:

Diffuser was designed to find the limit of maximum achievable mass flow at 5mm lift. But for that an optimized diffuser is needed such that it follows the gradual expansion. The outlet area of each diffuser is half of the port outlet area as in base geometry. The design is such that the length of the diffuser is around 150 mm and the angle of expansion is 6.5 degrees.
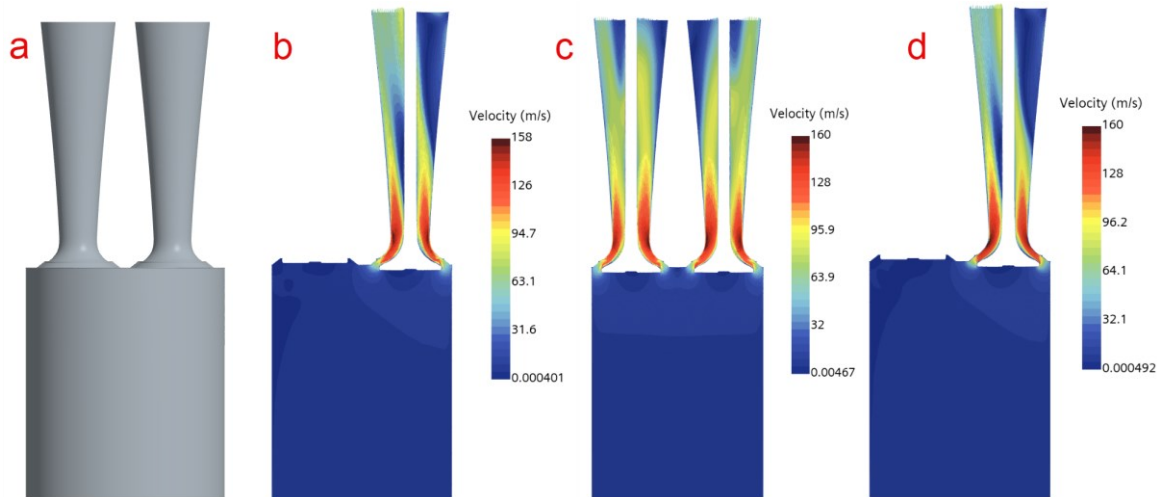
Figure 32 Diffuser flow at 5mm lift with length of 150mm a) geometry, b) flow viewed from left for left diffuser, c) flow viewed from front, d) flow viewed from left for right diffuser

With this diffuser mass flow at 5mm improved by approximately 36%. But fluctuations in the results were present which means the results may be not fully trusted. The backflow specification at the outlet was changed from extrapolated to boundary normal, and this made a huge change in terms of convergence of results.

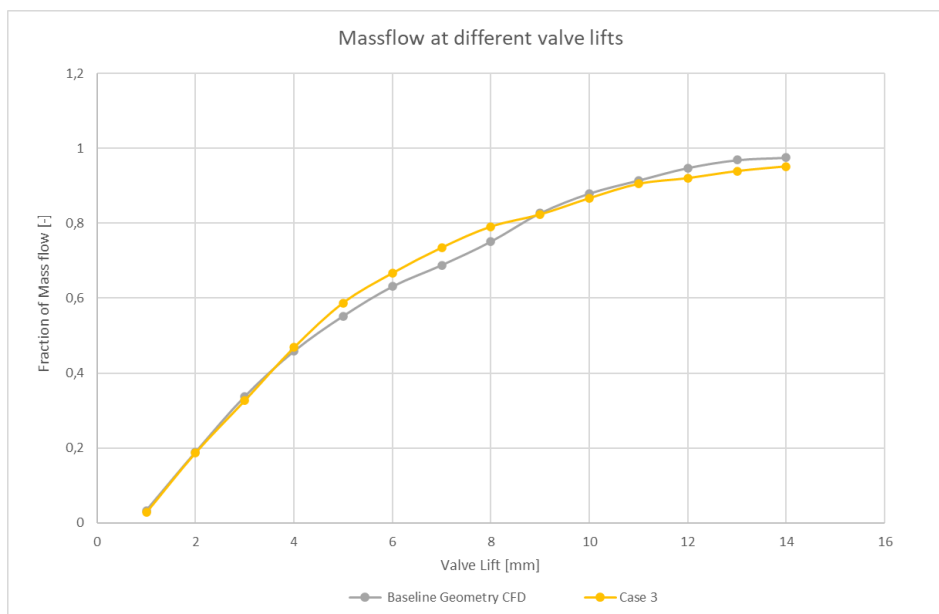A full sweep with the above diffuser design can be seen in figure 33.
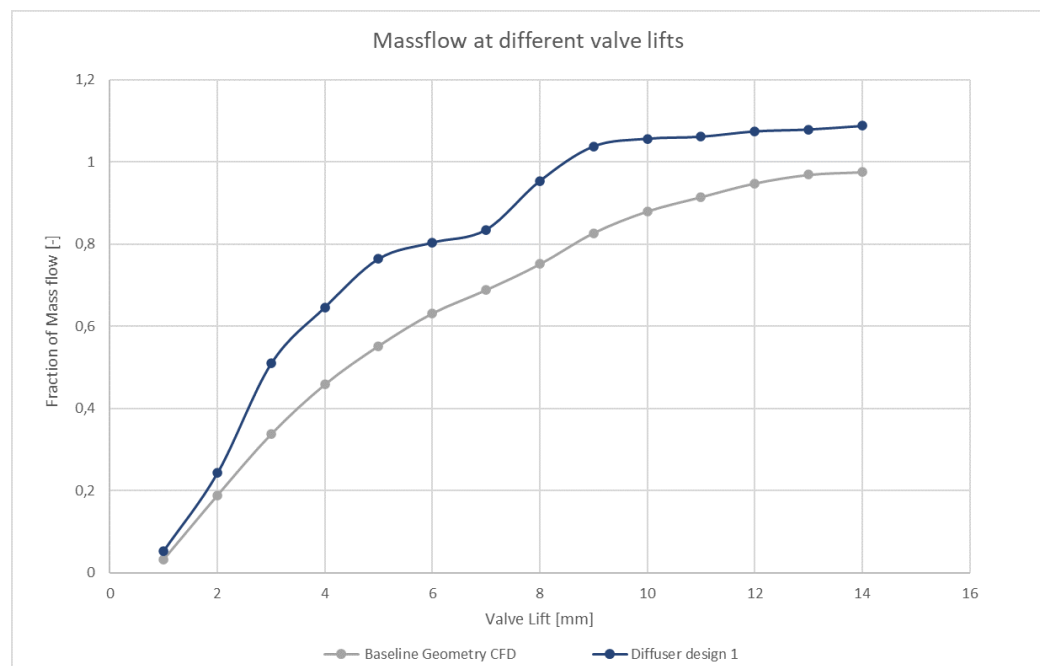
Figure 33 Mass flow as function of valve lift. Diffuser design 1 compared to simulation results.The massflow is expressed as fraction of the maximum flow in the flow test

But still the results from this diffuser design are not the best as it is not a smooth increase in the flow. This means that there were some errors with the simulation at those valve lifts and cannot be trusted completely.

9.2.2   Diffuser Design 2:

The same design principles were followed as previously, but the length of the tube is increased to 175 mm and the angle of expansion was reduced to 6 degrees to have a more subtle increase in expansion area. This case showed good improvement in mass flow compared to the diffuser design 1. The mass flow at 5mm valve lift was approximately 46% higher than the flow with base geometry at 5mm lift.
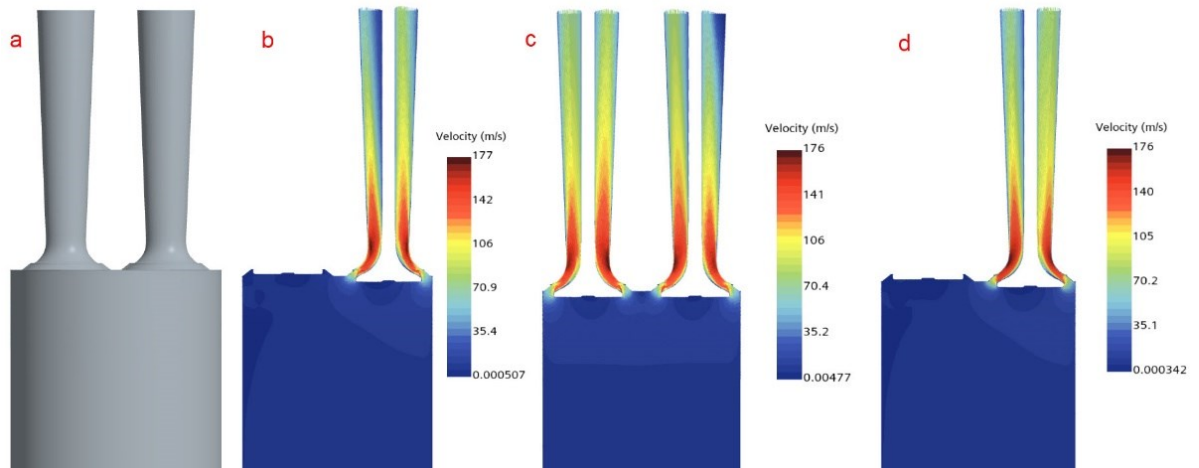
Figure 34 Diffuser flow at 5mm lift with length of 175 mm a) geometry, b) flow viewed from left for left diffuser, c) flow viewed from front, d) flow viewed from left for right diffuser.

A full sweep with the above diffuser design can be seen in figure 35.
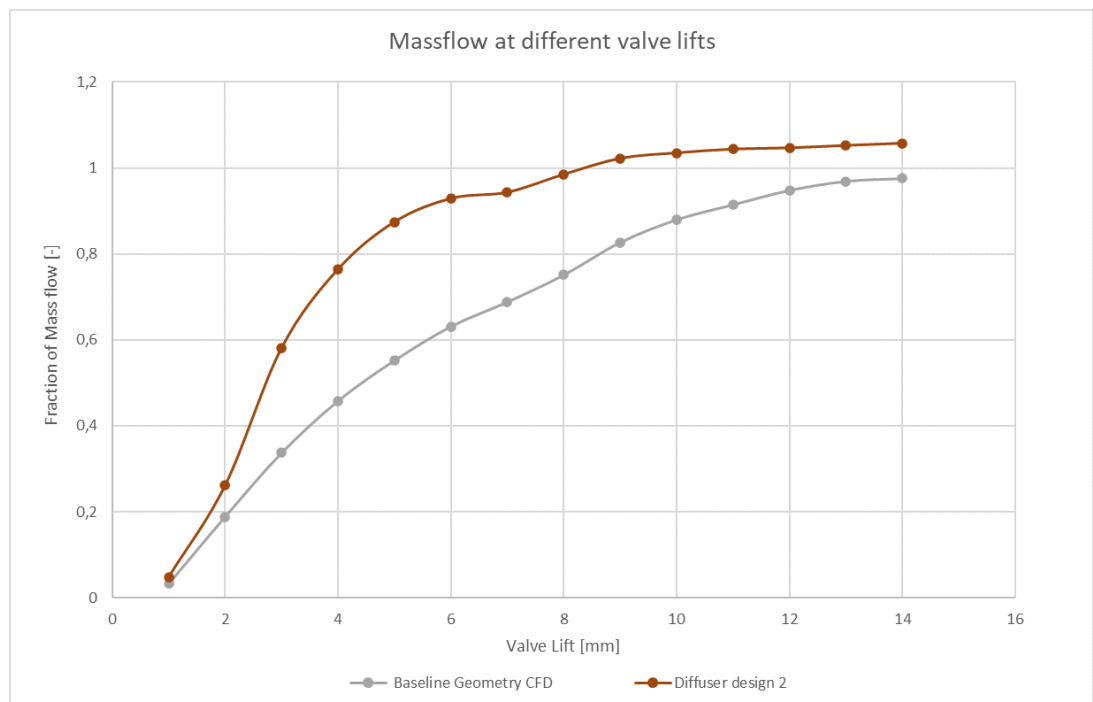
Figure 35 Mass flow as function of valve lift. Diffuser design 2 compared to simulation results. The mass flow is expressed as fraction of the maximum flow in the flow test.

## 9.3 Analysis of Efficiency:

Even though modifying the geometry made significant changes in the exhaust gas flow, the improvement in terms of efficiency need to be analyzed to see if the improved flow corresponds to improvement in efficiency. 1D performance simulation was performed with the CD values of each case at various operating points. This 1D simulation computes the efficiency, losses, engine power and many more parameters based on the given CD values. This gives an overall idea of the various changes that occur and determine if it improves the performance or not.

Two cases are considered which have the best improvement; case 3 where the port neck was modified and an improved flow of 5.3% was achieved and Diffuser Design 2 where an ideal diffuser was designed and an improvement of 46% in flow was achieved. These two cases are compared to the simulation result from CFD and the improvement in efficiency and losses are discussed below. The CD values of all these cases are used to compute the results of engine performance and with these results contour plots of BSFC, PMEP, Brake efficiency and thermodynamic efficiency are produced. The main aim of this section is to analyze the impact on the performance of the engine with respect to the improvements in the flow.

Five different comparisons are presented:

- 1D performance analysis of Base geometry compared to Case 3
- 1D performance analysis of Base geometry compared to Diffuser Design 2
- 1D performance analysis of Base geometry compared to Base geometry +10%
- 1D performance analysis of Diffuser Design 2 compared to Diffuser Design 2 + 10%
- 1D performance analysis of Base geometry (from CFD) compared to Test Results (measured from test)

The 1D simulation setup can be seen in figure 36. It is an in-house software used by Volvo and incorporates VGT (Variable Geometry Turbine) and EGR. In this the CD values from the CFD simulations are fed in the exhaust valve details seen near the pistons in figure 36.
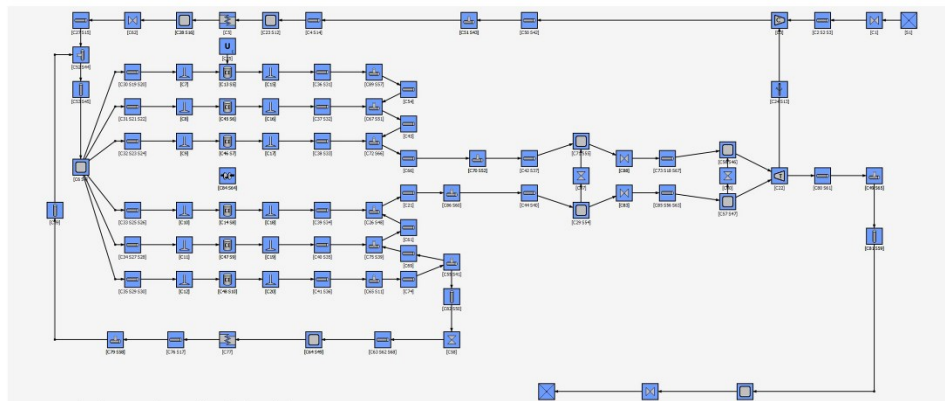
Figure 36 1D simulation setup used for performance analysis.

9.3.1   1D performance analysis of Base geometry compared to Case 3

The plots are created using 1D simulation and are plotted as a difference at each point in terms of percentage and it is calculated as (100*(case 3 – base geometry)/ base geometry) for BSFC, whereas for PMEP and efficiencies it is calculated as the absolute difference (case 3 – base geometry) since the efficiencies are already expressed in percentage. Even though case had an improved flow by 5.3% changes observed in BSFC and efficiencies was not

the best. BSFC is the amount of fuel consumed per unit of power output over a given time. Decrease in BSFC means lower fuel consumption and improved efficiencies. In figure 36 the plot for BSFC shows negative values in the white box, this indicates that bsfc for case 3 has lower values compared to base geometry. But this is not a significant change as the difference is lower than 0.01%. On the other hand, the PMEP has increased which indicates higher pumping losses and lower gas exchange efficiencies. As expected, with a significantly small improvement in bsfc, the efficiency also follows a similar pattern of small increments. The thermodynamic and brake efficiency is almost zero which indicates no improvements.
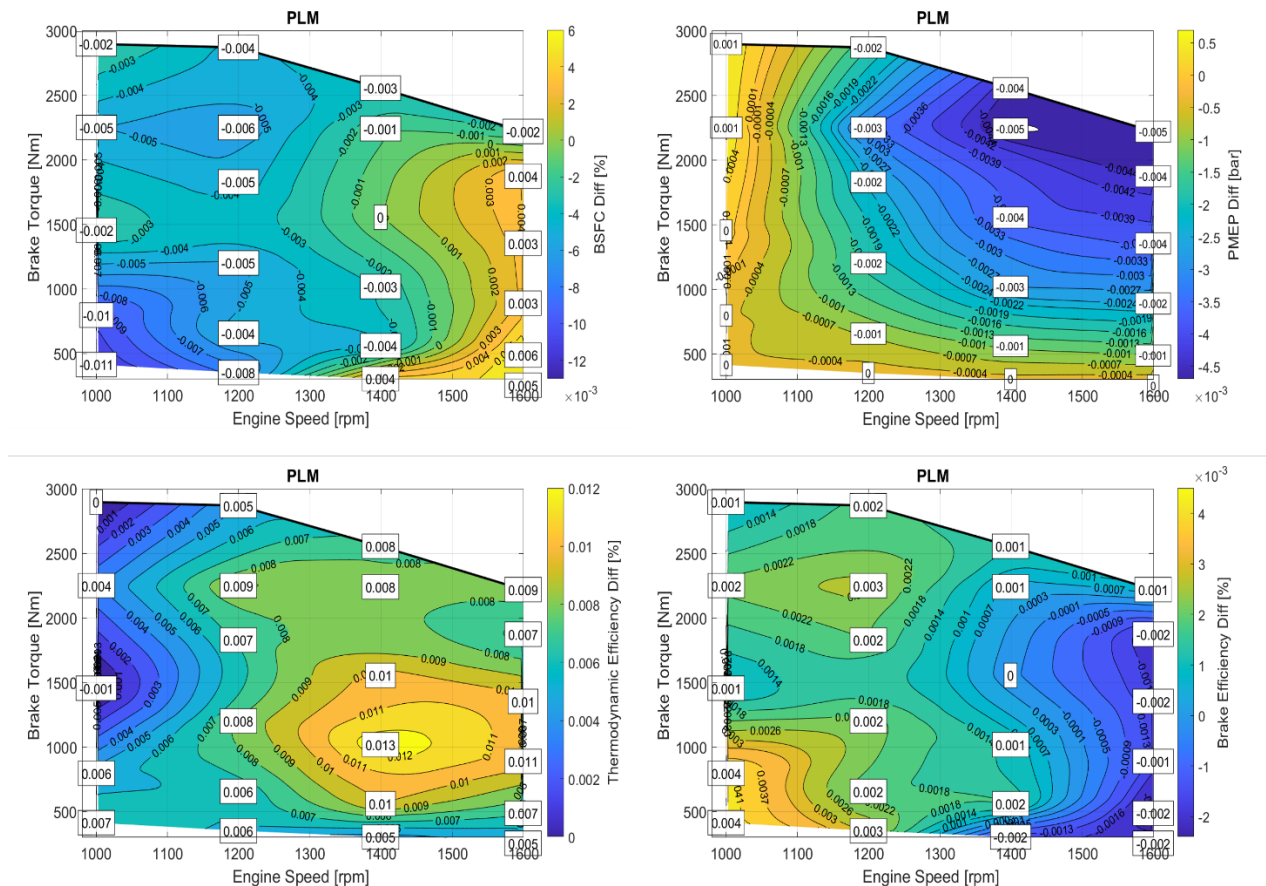
Figure 37 BSFC plotted as a percentage difference calculated as (100*(case 3 – base geometry)/ base geometry). PMEP, Thermodynamic and Brake efficiency plotted as absolute difference calculated as (case 3 – base geometry).

9.3.2   1D performance analysis of Base geometry compared to Diffuser Design 2

The plots are created as a difference at each point in terms of percentage and it is calculated as (100*(Diffuser design 2 – Base geometry)/ Base geometry) for BSFC, whereas for PMEP and efficiencies it is calculated as the absolute difference (case 3 – base geometry). With the improvement of 46% in flow by using an ideal diffuser, good improvements can be observed both in efficiencies and bsfc. The plot on the top left in figure 37 shows bsfc plotted as difference against speed and torque, and the value in the white box indicates the improved bsfc for diffuser design 2 compared to base geometry. PMEP shows negative values which indicate that the diffuser design 2 has reduced pumping losses which indicates improved gas exchange efficiency. Even with good improvement with bsfc, the

improvement in efficiencies is still significantly low. However, it is comparatively better than the previous case.

Figure 38 BSFC plotted as a percentage difference calculated as (100(Diffuser design 2 – Base geometry)/ Base geometry). PMEP, Thermodynamic and Brake efficiency plotted as absolute difference calculated as (diffuser design 2 – base geometry).*

9.3.3 1D performance analysis of Base geometry compared to Base geometry +10%

The plots are created as a difference at each point in terms of percentage and it is calculated as (100*(Base geometry +10% – Base geometry)/ Base geometry) for BSFC, whereas for PMEP and efficiencies it is calculated as the absolute difference (case 3 – Base geometry) shown in figure 38. Here '+10%' indicate that the CD values for the base geometry are increased by 10%, this is done by increasing the effective area in equation 2. With this the improvement in bsfc, pmep and efficiencies are better that case 3 and to an extent similar to diffuser design 2. However, the difference can be seen for thermodynamic efficiency which indicates that the base geometry has quite some heat losses even if the effective flow area is increased.

Figure 39 BSFC plotted as a percentage difference calculated as (100*(Base geometry +10% – Base geometry)/ Base geometry). PMEP, Thermodynamic and Brake efficiency plotted as absolute difference calculated as (base geometry (+10%) – base geometry).

9.3.4   1D performance analysis of Diffuser Design 2 compared to Diffuser Design 2 + 10%

The plots are created as a difference at each point in terms of percentage and it is calculated as (100*(Diffuser design 2 +10% – diffuser design 2)/ diffuser design 2) for BSFC, whereas for PMEP and efficiencies it is calculated as the absolute difference (case 3 – simulation results) shown in figure 39. Same as before the 10% indicate the CD values are increased by 10% by increasing the effective flow area. When the flow area is increased by 10% the bsfc and the efficiencies also increase by a certain percent. Flow area proves to play a significant role in improving efficiencies and reducing losses.
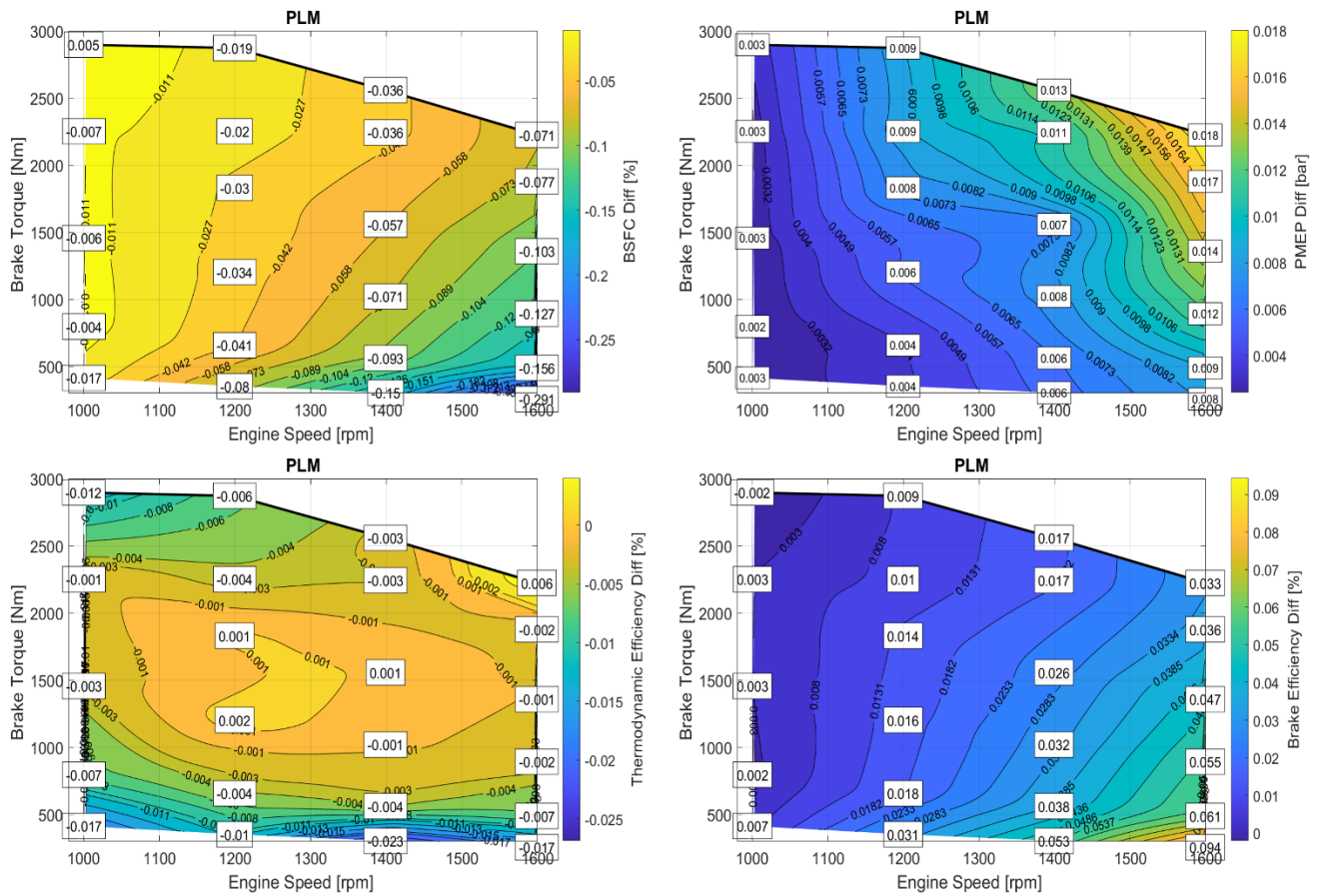
Figure 40 BSFC plotted as a percentage difference calculated as (100(diffuser design (+10%) - diffuser design)/diffuser design). PMEP, Thermodynamic and Brake efficiency plotted as absolute difference calculated as (diffuser design (+10%) - diffuser design).*

9.3.5 1D performance analysis of Base geometry (from CFD) compared to Test results

The plots are created as a difference at each point in terms of percentage and it is calculated as (100*(Test result– Base geometry)/ Base geometry) for BSFC, whereas for PMEP and efficiencies it is calculated as the absolute difference (test results – Base geometry) shown in figure 40. From figure 14 it was clear that there some difference between the base geometry and test results. This comparison was done to see how this difference affects the bsfc and efficiencies. Figure 44 shows the difference in efficiencies and bsfc due to the difference in base geometry in comparison to test results.

39
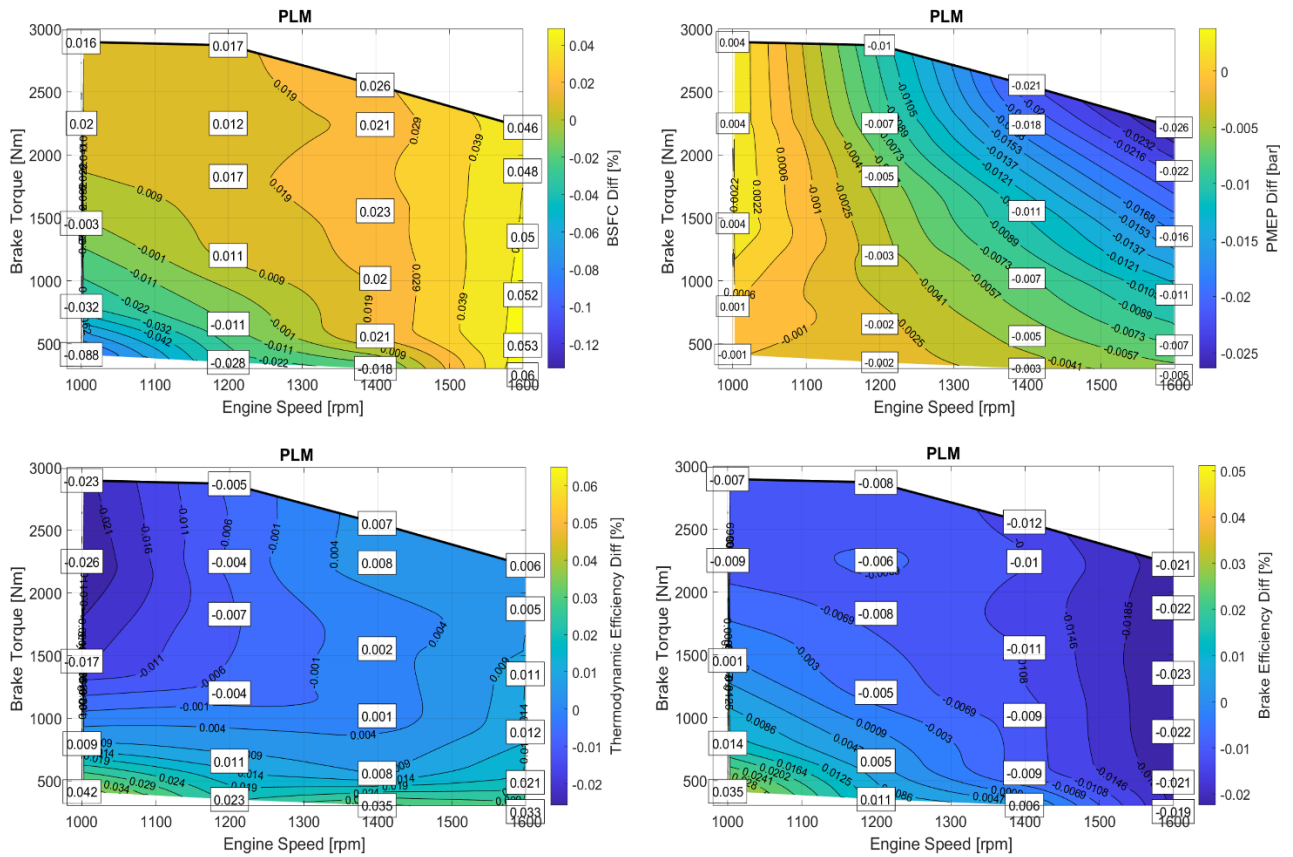
Figure 41 BSFC plotted as a percentage difference calculated as (100(Test result– Base geometry)/ Base geometry). PMEP, Thermodynamic and Brake efficiency plotted as absolute difference calculated as (test results – Base geometry).*

9.3.6 Conclusion

In conclusion from the analysis of efficiency, improving the exhaust gas flow does lead to improvement in engine performance, but the improvement is comparatively low. It is also clear that even with a good improvement in bsfc there is not much improvement in the efficiencies. This indicates that improving the exhaust gas flow can improve the bsfc, however it does not correspond to the same level of improvement in efficiency. On the other hand, improving the CD values by 10% also had some improvements, which suggests that increasing the effective flow area can also support to improvements in efficiency.

10.   Discussion

Even with this results there are lots of points that have ignored for simplicity. In an ideal simulation condition it is ok to have lower boundary values (in this case 106.3 and 101.3 kPa) but this is not the same when it comes to real time operating of ICE. This done to simplify complex physical processes for computational feasibility and ensure that simulation can be completed within a respected time frame.

Another thing to consider is simulation flow setup varies from real engine flow setup. The simulation follows a static flow setup whereas in real engine the flow is dynamic. In an actual engine there is heat transfer between the combustion chamber, walls and the cooling system which is complex. In a static CFD simulation fixed temperatures or heat flux for walls as a boundary condition are assumed which leads to inability to capture transient thermal interaction which are visible in real engines.

Finally in this thesis the optimization is mainly focused on intermediate valve lifts (5mm-7mm). But this is not the best ideology theoretically. Optimizing at lower valve lifts are seen to contribute more in improving engine performance and efficiency as well. At lower valve lifts is where most of the scavenging (expelling of exhaust gases) occurs and it is important to improve the scavenging efficiency to have reduced pumping losses. It is understood that improving the scavenging efficiency can ultimately contribute to better flow and reduced pumping losses when optimized at lower valve lifts.

11.   Conclusion and Future Work

The following conclusions are drawn based on the literature study and simulation results:

- It is evident from literature review that there are certain losses that occur due to improper exhaust flow. This can be improved by making modifications to the port geometry. Among the various strategies, modifying the port area above the throat area seemed the most effective in terms of improving flow as well as reduced losses. To analyze this flow a CFD simulation must be performed which uses turbulence models to predict the flow accurately. From the various types of turbulence models RANS seems to be the most suited for this thesis as it has become an industry standard for flow simulations. Additionally, a diffuser design is also analyzed to understand the maximum achievable exhaust flow.
- In RANS there are two major turbulence models namely the k-epsilon and k-omega. Initially k-epsilon model was tried for the geometry, but this model displayed poor convergence at some valve lifts which indicate that the results cannot be trusted entirely. On the other hand, k-omega model displayed good convergence which became the choice for further simulations as well.
- Among the various available optimization strategies two of them were found suitable for this thesis, one is the adjoint solver which predicts the parameters that influence the target and modifies the geometry accordingly, another is parameter optimization which involves making changes to parameters like diameter, angle, area and so on manually to see its effect on the target required. Out of this parameter optimization was the method chosen since adjoint solver method posed complications and strange results with the restriction in the geometry at valve seats.
- With the base geometry four cases were tried where case 1 had valve face in line with the cylinder head, case 2 had valve inside the combustion chamber, case 3 had modified port neck area and case 4 had smoothened valve edge along with reduced port neck area. Among these cases 3&4 showed the best improvement in flow by 5.3% and 6.9% compared to flow with the base geometry. However, case 4 poses a complication in reduced valve seat area which reduces the contact area and reduces heat dissipation capacity.
- Additionally, two diffuser designs were analyzed with different lengths for each diffuser design, the diffuser with the shorter length of 150mm showed an improved flow by 36%, and another diffuser with length of 175mm showed an improved flow by 46%.
- 1D performance analysis of the efficiency show that even with an improved flow of 46%, the improvement in efficiency only corresponds to about less than 0.1%. However, increasing the CD number by increasing the effective flow area can lead to a slightly higher improvement in the efficiency.
- Finally, it can be concluded that if the valve diameter and valve seat area are modified, there could be chances of improving the flow and thus the efficiencies as well.

Future works include:

- Even though the diffuser design shows a significant improvement in flow, the flow behavior will change drastically when the port is bent. The performance of the port must be optimized when it is bent.

- After that, a prototype will be produced and a full engine test under various operating conditions would be evaluated in a test bench setup to analyze the losses, emissions, and engine efficiency as well.

12.   References

- Blevins, Robert D (1984). "Applied fluid dynamics handbook". In: New York.
- "Chapter 3 - Contraction and Expansion Flows" (1993). In: Boger, D. et al. (Eds.). Rheological Phenomena in Focus. Vol. 4. Rheology Series. Elsevier, pp. 35–72. DOI: https://doi.org/10.1016/B978-0-444-89473-1.50008-8. URL: https: / / www. sciencedirect . com / science / article / pii /B9780444894731500088.
- Cengel, Y. A., M. A. Boles, and M. Kanoğlu (2011). Thermodynamics: an engineering approach. Vol. 5. McGraw-hill New York.
- Dixon, S. L. and C. Hall (2013). Fluid mechanics and thermodynamics of turbomachinery. Butterworth-Heinemann.
- Gülmez, Y. and G. Özmen (2021). "Effects of exhaust backpressure increment on the performance and exhaust emissions of a single cylinder diesel engine." Journal of ETA Maritime Science 9:3.
- Heywood, J. B. (1988). Internal combustion engine fundamentals. Mcgraw-hill.
- Hires, S. and G. Pochmara (1976). "An analytical study of exhaust gas heat loss in a piston engine exhaust port". SAE Transactions, pp. 2415–2429.
- Holmberg, T., A. Cronhjort, and O. Stenlaas (2017). Pressure ratio influence on exhaust valve flow coefficients. Tech. rep. SAE Technical Paper.
- Hopf, A. (2022). "Cfd topology and shape optimization of twin ports in integrated exhaust manifolds". SAE International Journal of Advances and Current Practices in Mobility 5:2022-01-0785, pp. 181–193.
- Majewski, W. and H. Jääskeläinen (2023). Diesel Emissions and Their Control, 2nd Edition. SAE International. ISBN: 9781468605709. URL: https: / / books google.se/books?id=mnrsEAAAQBAJ.
- Rai, S., S. Arslan, and B. Jawad (2018). Exhaust heat recovery system study in internal combustion engines. Tech. rep. SAE Technical Paper.
- Semlitsch, B., Y. Wang, and M. Mihãescu (2015). "Flow effects due to valve and piston motion in an internal combustion engine exhaust port". Energy Conversion and Management 96, pp. 18–30
- Singh, A., S. Poonia, A. Jalan, J. Singh, and N. Kumar (2019). Intake and Exhaust Ports Design for Tumble and Mass Flow Rate Improvements in Gasoline Engine. Tech. rep. SAE Technical Paper.
- Tu, J., G. H. Yeoh, C. Liu, and Y. Tao (2023). Computational fluid dynamics: a practical approach. Elsevier.
- Wang, X., J. Ma, and H. Zhao (2018). "Analysis of scavenge port designs and exhaust valve profiles on the in-cylinder flow and scavenging performance in a two-stroke boosted uniflow scavenged direct injection gasoline engine". International Journal of Engine Research 19:5, pp. 509–527.
- Wang, Y. (2013). Numerical Studies of Flow and Associated Losses in the Exhaust Port of a Diesel Engine. PhD thesis. KTH Royal Institute of Technology.

- Wang, Y., B. Semlitsch, M. Mihaescu, and L. Fuchs (2013). "Flow structures and losses in the exhaust port of an internal combustion engine". 56314, V07AT08A045.
- Wang, Y., B. Semlitsch, M. Mihaescu, and L. Fuchs (2015). "Flow induced energy losses in the exhaust port of an internal combustion engine". Journal of Fluids Engineering 137:1, p. 011105.
- Wang, Z., S. Shuai, Z. Li, and W. Yu (2021). "A review of energy loss reduction technologies for internal combustion engines to improve brake thermal efficiency". Energies 14:20, p. 6656.
- Xu, Y., S. Huang, L. Su, X. Zhang, and Y. Li (2022). "Elbow flow analysis and optimal exhaust port profile design". Journal of Mechanical Science and Technology 36:3, pp. 1251–1262.
- Xu, Y., F. Liu, Y. Hua, J. Rui, and Y. Li (2019). Influence of key section parameters of exhaust port on flow capacity. Tech. rep. SAE Technical Paper.
- Zirngibl, S., S. Held, M. Prager, and G. Wachtmeister (2017). Experimental and simulative approaches for the determination of discharge coefficients for inlet and exhaust valves and ports in internal combustion engines. Tech. rep. SAE technical paper.